SCIENCE CHINA
Information Sciences

• RESEARCH PAPER •

March 2025, Vol. 68, Iss. 3, 132208:1–132208:19
https://doi.org/10.1007/s11432-023-4299-7

Distributed stochastic source seeking and formation control based on delayed measurements

Pei-Pei ZHANG[1,2], Lin-Yu YANG[1] & Shu-Jun LIU[1*]

[1]*School of Mathematics, Sichuan University, Chengdu 610064, China*
[2]*School of Data and Computer Science, Shandong Women's University, Jinan 250300, China*

Received 15 July 2023/Revised 15 September 2024/Accepted 27 October 2024/Published online 13 February 2025

Abstract In this paper, we design a distributed stochastic source seeking algorithm based on time-delay measurements to implement source seeking and formation control, so that vehicles can achieve and maintain a specific formation during the source seeking process. First, we present continuous-time stochastic averaging theorems for nonlinear delay-differential systems with stochastic perturbations. Then, based on the stochastic extremum seeking method and the leaderless formation strategy, we design a distributed stochastic source seeking algorithm based on time-delay measurements to navigate multiple velocity-actuated vehicles to search for an unknown source while achieving and maintaining a predefined formation, and the effect of the delay is eliminated by adopting the one-stage sequential predictor approach. Moreover, based on our developed stochastic averaging theorems, we prove that the average position of vehicles exponentially converges to a small neighborhood of the source in the almost sure sense, and vehicles can achieve and maintain a predefined formation. Finally, we provide numerical examples to verify the effectiveness of our proposed algorithm.

Keywords distributed source seeking, formation control, stochastic extremum seeking, stochastic averaging, time delays

Citation Zhang P-P, Yang L-Y, Liu S-J. Distributed stochastic source seeking and formation control based on delayed measurements. Sci China Inf Sci, 2025, 68(3): 132208, https://doi.org/10.1007/s11432-023-4299-7

1 Introduction

Distributed source seeking, in which multiple agents cooperate with their neighbors through a communication topology and move toward an unknown source, has received much attention [1–4]. The source considered here can emit some signals in the environment, such as smell, concentration, temperature, and light intensity, and locate at the maximum strength of such signals. Generally speaking, the spatial distribution of the signal field is hard to obtain, and only measurements of the signal strength can be used. To complete the source seeking task, the gradient of the scalar signal field is estimated by different methods: stochastic extremum seeking method [3, 4], stochastic approximation method [1], least squares method [2], and for different communication topologies, fixed topology [1–3], switching topology [4].

Formation control, aiming to design a proper controller to drive multiple agents to achieve a desired formation and maintain this formation during their movement, has been studied intensively [5–14]. Since a formation is beneficial for reducing air resistance, achieving reliable communication, and ensuring safety in hazardous environments, the formation control has been applied to source seeking problems [15–22]. The focus of these studies is on how to make a group of agents achieve and maintain a predefined formation during the process of source seeking. There are two schemes to solve this problem: leader-follower scheme [15–17, 19, 20] and leaderless scheme [18, 21, 22]. In the leader-follower scheme, at least one virtual or real agent acts as the leader and the others are followers, and the leader can influence the states of the followers but not vise versa, and the followers track the leader with keeping some desired offsets while the leader performs the source seeking task. In the leaderless scheme, agents cooperatively perform source seeking tasks while achieving and maintaining a predefined formation. To complete the source seeking tasks, the gradient of the scalar signal field is estimated by different methods, such as deterministic extremum seeking method [15], least squares method [16, 17, 21, 22], weighted least squares method [18], and weighted average method [19, 20]. Unlike gradient estimation algorithms in [16–22],

* Corresponding author (email: sjliu@scu.edu.cn)

in which each agent needs signal measurement information from its neighbors, in the extremum seeking algorithm each agent needs only its own signal measurement information (e.g., [15]). All these studies consider the case of real-time measurements without time delays.

Based on time-delay measurements, some deterministic extremum seeking algorithms (e.g., [23–25]) adopt two typical compensation approaches to eliminate the effect of time delays. Specifically speaking, the first approach, known as the forwarding-backstepping transformation approach, uses a state of an integro-differential system to compensate for time delays [23, 24], while the other one, known as the one-stage sequential predictor approach, uses a state of a differential-difference system [25]. Moreover, in [24, 26], some stochastic extremum seeking algorithms are given based on time-delay measurements, where the forwarding-backstepping transformation approach is introduced to compensate for time delays. For the convergence analysis of the algorithms in [24, 26], the stochastic averaging theorem from [27] is used, and the theorem is established about moment convergence under the globally Lipschitz condition and the zero equilibrium condition. Besides, some other stochastic averaging theorems for delayed systems are established under different conditions, including the moment convergence results under the globally Lipschitz condition [28], and the weak convergence results under the locally Lipschitz condition and the linear growth condition [29]. To the best of our knowledge, there is no stochastic averaging result (especially in the almost sure sense) for nonlinear time-delay systems without the linear growth condition.

In this paper, based on time-delay measurements, we consider designing a distributed stochastic source seeking algorithm to drive vehicles to achieve and maintain a predefined formation while moving toward an unknown signal source. First, to analyze the convergence of the distributed stochastic source seeking algorithm, we develop stochastic averaging theorems for a class of locally Lipschitz nonlinear time-delay systems with stochastic perturbations. Then, considering that the leader-follower scheme is overly dependent on the leader for implementing the source seeking tasks, and that over-dependence on a single agent in the formation may not be desired [30], we apply the stochastic extremum seeking method and the leaderless formation control strategy to design our algorithm based on time-delay measurements to tune the velocity inputs of multiple velocity-actuated vehicles, such that the vehicles can achieve a predefined formation while seeking the unknown signal source and ultimately keep this formation moving around the signal source. In addition, to eliminate the effect of the delay on the convergence of the distributed stochastic source seeking algorithm, the one-stage sequential predictor approach is adopted instead of the forwarding-backstepping transformation approach due to its advantage of high efficiency computation [25]. Moreover, based on our developed stochastic averaging theorems, we prove that the vehicles can achieve a predefined formation during the source seeking process and their averaging position exponentially converges to a small neighborhood of the signal source in the almost sure sense, which enables the vehicles eventually to move around the signal source in such a formation.

The main contributions of our work can be summarized as follows. (i) Stochastic averaging theorem is established in the almost sure sense for locally Lipschitz nonlinear time-delay differential systems with stochastic perturbations. (ii) A distributed stochastic source seeking algorithm based on time-delay measurements is presented including its rigorous convergence proof. (iii) The application of formation control to the distributed source seeking not only makes it possible to ensure reliable communication and reduce the energy consumption of vehicles during the source seeking process, but also effectively avoids collisions of vehicles around the source.

The rest of the paper is organized as follows. Section 2 gives problem formulation. Section 3 shows stochastic averaging theorems for nonlinear time-delay systems with stochastic perturbations. Section 4 presents the distributed stochastic source seeking algorithm and its convergence analysis. Section 5 provides some numerical simulations to verify the effectiveness of our proposed algorithm. Section 6 makes some concluding remarks. Appendixes A–C give some proofs of the main results.

Notation. $\mathbb{R}^n$ is the real n-dimensional space. For $x \in \mathbb{R}^n$, x^{T} is its transpose. $\operatorname{diag}\{a_1, a_2, \dots, a_n\}$ is an n-order diagonal matrix whose principal diagonal elements are a_i, $i \in \{1, 2, \dots, n\}$. I_n is an identity matrix of order n. $\mathbf{1}_n$ is an n-dimensional column vector of ones. $\lambda_{\min}(S)$ is the smallest eigenvalue of the matrix S. $\mathscr{C}_n = C([-D, 0]; \mathbb{R}^n)$ is the space of continuous functions $\varphi : [-D, 0] \to \mathbb{R}^n$ with the norm $\|\varphi\| = \sup_{\theta \in [-D,0]} |\varphi(\theta)|$, where $|x|$ is the Euclidean norm of the column vector x. For $a, b \in \mathbb{R}$, $a \wedge b = \min\{a, b\}$, and $a \vee b = \max\{a, b\}$. $\otimes$ is the Kronecker product.

2 Problem formulation

We consider a multi-agent system composed of N velocity-actuated vehicles that are in a scalar signal field. The spatial distribution of the signal field is described by a map $f(x):\mathbb{R}^2\to\mathbb{R}$, which has an isolated local maximum point x^* corresponding to the location of the signal source. The explicit expression of the spatial distribution $f(x)$ is often unknown, but the vehicles can obtain measurements of the scalar signal field at their own positions. To search for the source cooperatively, the vehicles communicate in real time through a connected undirected graph $\mathcal{G}=\{\mathcal{V},\mathcal{E},A,\mathcal{L}\}$ with vertex set $\mathcal{V}=\{1,2,\ldots,N\}$, edge set $\mathcal{E}\subseteq\mathcal{V}\times\mathcal{V}$, adjacency matrix $A=[a_{ij}]_{N\times N}$, and Laplacian matrix $\mathcal{L}=[l_{ij}]_{N\times N}$, where

$$a_{ij}=\begin{cases}a_{ji}>0, & (i,j)\in\mathcal{E},\\ 0, & (i,j)\notin\mathcal{E},\end{cases}\quad\text{and}\quad l_{ij}=\begin{cases}\sum_{k=1,k\neq i}^{N}a_{ik}, & i=j,\\ -a_{ij}, & i\neq j.\end{cases}$$

For $i\in\mathcal{V}$, the kinematics of vehicle i is formulated as

$$\dot{x}_i=v_i, \tag{1}$$

where $x_i\in\mathbb{R}^2$ and $v_i\in\mathbb{R}^2$ are the position and velocity inputs of the ith vehicle center in the plane, respectively. Vehicle i can measure its relative position to its neighbor vehicle j but cannot access its absolute position, where $j\in\mathcal{N}_i$ and $\mathcal{N}_i=\{j\in\mathcal{V}:(i,j)\in\mathcal{E}\}$ is the set of neighbors of vehicle i.

Considering that time delays often occur in the actual information measurement process, here we consider a known constant measurement delay $D>0$. In this case, each vehicle cannot obtain the signal measurement information of its current position, nor measurements of its current relative positions to its neighbors, but only their historical measurements delayed by D time units can be obtained. Our goal is to design a distributed stochastic source seeking algorithm based on the delayed measurements to tune the velocity inputs of the vehicles such that they can achieve a predefined formation while seeking an unknown signal source, and ultimately keep this formation moving around the signal source. Since the formation is predefined, it is reasonable to assume that each vehicle knows the formation information.

Definition 1. ([5]) Let $h=(h_1^{\mathrm{T}},h_2^{\mathrm{T}},\ldots,h_N^{\mathrm{T}})^{\mathrm{T}}\in\mathbb{R}^{2N}$ denote a specified formation. For multi-agent system (1), the desired formation h is said to be achieved if for some appropriate initial states,

$$\lim_{t\to+\infty}\big(x_i(t)-x_j(t)-h_i+h_j\big)=0,\quad\forall i,j\in\mathcal{V}, \tag{2}$$

where h_i-h_j denotes the desired relative position between vehicles i and j.

For any fixed $i\in\mathcal{V}$, according to (2), we obtain $\lim_{t\to+\infty}\frac{1}{N}\sum_{j=1}^{N}(x_i(t)-x_j(t)-h_i+h_j)=0$, which means

$$\lim_{t\to+\infty}\big(x_i(t)-c(t)-h_i+h^*\big)=0,\quad\forall i\in\mathcal{V}, \tag{3}$$

where $h^*=\frac{1}{N}\sum_{j=1}^{N}h_j$ denotes the mean center of the desired formation h, and $c(t)=\frac{1}{N}\sum_{j=1}^{N}x_j(t)$ denotes the average position of the vehicles. In turn, we can also get (2) from (3), so Eq. (2) is equivalent to (3). By (3), it can be obtained that as time goes by, the offset of vehicle i from the average position $c(t)$ tends to h_i-h^*, and the relative position between vehicles i and j tends to h_i-h_j. If we can drive the vehicles such that their average position $c(t)$ tends to the signal source, then the vehicles can ultimately keep moving around the source in this formation h. Therefore, based on time-delay measurements, we can achieve our goal by designing a distributed stochastic source seeking algorithm such that Eq. (3) holds and their average position $c(t)$ converges to a small neighborhood of the signal source.

Remark 1. When $c(t)$ converges to a small neighborhood of the signal source x^*, we obtain that $x_i(t)-x^*-h_i+h^*$ converges to a small neighborhood of zero by (3), which means that there is an offset h_i-h^* between the vehicle i and the signal source x^*. Therefore, in order to ensure that vehicle i can be closer to the signal source, h_i-h^* should not be too large in the subsequent algorithm design process. In addition, h_i-h_j should meet the actual demands of communication and safety between vehicles i and j.

Remark 2. In this paper, we focus on distributed source seeking and formation control based on delayed measurements, including the development of analysis tool and algorithms designed for the case with a known constant time delay. For actual information measurement process, multiple time delays may arise. They may be distinct, time-varying, or even unknown [31]. For these cases, we can design stochastic extremum seeking algorithms by adjusting the algorithm proposed in this paper, but it is difficult to prove their convergence because of the lack of theoretical analysis tools. New extended stochastic averaging theorems need to be developed to prove the convergence of the stochastic extremum seeking algorithms which can solve optimization problems with distinct, time-varying, or even unknown time delays. This is also our next research direction.

3 Analysis tool: stochastic averaging for nonlinear time-delay systems

Since we consider designing the stochastic extremum seeking algorithm based on delayed measurements, the system to be analyzed is a nonlinear system with time delay and stochastic perturbations. For this class of systems, in this section we develop stochastic averaging theorems for the subsequent theoretical analysis.

Consider the following delay-differential system:

$$\frac{\mathrm{d}X^\epsilon(t)}{\mathrm{d}t} = f(X^\epsilon(t), X^\epsilon(t-D), Y_1(t/\epsilon_1), Y_2(t/\epsilon_2), \ldots, Y_l(t/\epsilon_l)), \quad t>0, \tag{4}$$

$$X^\epsilon(t) = X_0(t), \quad \forall t\in[-D,0], \tag{5}$$

where $X^\epsilon(t)\in\mathbb{R}^n$ is the system state, and $Y_i(t)\in\mathbb{R}^{m_i}$, $1\leqslant i\leqslant l$ are the perturbation processes defined on a complete probability space $(\Omega,\mathcal{F},P)$ with the sample space Ω, the σ-field $\mathcal{F}$, and the probability measure P. $D>0$ is a constant delay. The initial condition $X_0(t):[-D,0]\to\mathbb{R}^n$ is a deterministic continuous function, i.e., $X_0(t)\in\mathscr{C}_n$. The small parameters ϵ_i, $1\leqslant i\leqslant l$ belong to $(0,\epsilon_0)$ for a constant $\epsilon_0>0$, and $\epsilon=[\epsilon_1,\epsilon_2,\ldots,\epsilon_l]^{\mathrm{T}}$. Let S_{Y_i} denote the living space of the perturbation process $(Y_i(t),t\geqslant 0)$, and it is a proper subset of $\mathbb{R}^{m_i}$.

Let $\epsilon_i=\frac{\epsilon_1}{c_i}$, $i\in\{2,\ldots,l\}$ with $c_i>0$. Let $Z_1(t)=Y_1(t)$, $Z_i(t)=Y_i(c_it)$, $i\in\{2,\ldots,l\}$, and $Z(t)=\left[Z_1^{\mathrm{T}}(t),\ldots,Z_l^{\mathrm{T}}(t)\right]^{\mathrm{T}}$. Then Eqs. (4) and (5) become

$$\frac{\mathrm{d}X^{\epsilon_1}(t)}{\mathrm{d}t} = f(X^{\epsilon_1}(t), X^{\epsilon_1}(t-D), Z(t/\epsilon_1)), \quad t>0, \tag{6}$$

$$X^{\epsilon_1}(t) = X_0(t), \quad \forall t\in[-D,0], \tag{7}$$

where $X^{\epsilon_1}(t)=X^\epsilon(t)$ and $Z(t/\epsilon_1)=\left[Z_1^{\mathrm{T}}(t/\epsilon_1),\ldots,Z_l^{\mathrm{T}}(t/\epsilon_1)\right]^{\mathrm{T}}$.

We consider the following assumptions.

Assumption 1. $f(x_1,x_2,y_1,y_2,\ldots,y_l):\mathbb{R}^n\times\mathbb{R}^n\times S_{Y_1}\times S_{Y_2}\times\cdots\times S_{Y_l}\to\mathbb{R}^n$ is a continuous function of $(x_1,x_2,y_1,y_2,\ldots,y_l)$. For all $x_1,x_2\in\mathbb{R}^n$, $f(x_1,x_2,\cdot)$ is a bounded function of $y=[y_1^{\mathrm{T}},y_2^{\mathrm{T}},\ldots,y_l^{\mathrm{T}}]^{\mathrm{T}}$. Meanwhile, it satisfies the locally Lipschitz condition in (x_1,x_2) uniformly in $y\in S_{Y_1}\times S_{Y_2}\times\cdots\times S_{Y_l}$, that is, for all $c>0$, there exists a constant $L_c>0$ such that for all $|x_1|\vee|x_2|\vee|\check{x}_1|\vee|\check{x}_2|\leqslant c$, for all $y\in S_{Y_1}\times S_{Y_2}\times\cdots\times S_{Y_l}$,

$$|f(x_1,x_2,y)-f(\check{x}_1,\check{x}_2,y)|\leqslant L_c(|x_1-\check{x}_1|+|x_2-\check{x}_2|).$$

Assumption 2. For any $X_0(t)\in\mathscr{C}_n$ and the stochastic process $(Z(t),t\geqslant 0)$, system (6) and (7) has a unique solution on $[-D,+\infty)$ in the almost sure sense.

Assumption 3. The independent perturbation processes $(Y_i(t),t\geqslant 0)$, $i\in\{1,2,\ldots,l\}$ are ergodic with invariant distribution μ_i, respectively.

Based on the Lemmas 8.1 and 8.2 in [32], the process $(Z(t),t\geqslant 0)$ is ergodic with the invariant distribution $\mu_1\times\mu_2\times\cdots\times\mu_l$. Then, we can define the average system of system (6) and (7) as follows:

$$\frac{\mathrm{d}\bar{X}(t)}{\mathrm{d}t} = \bar{f}(\bar{X}(t),\bar{X}(t-D)), \quad t>0, \tag{8}$$

$$\bar{X}(t) = X_0(t), \quad \forall t\in[-D,0], \tag{9}$$

where

$$\bar{f}(x_1,x_2)=\int_{S_{Y_1}\times S_{Y_2}\times\cdots\times S_{Y_l}} f(x_1,x_2,z_1,z_2,\ldots,z_l)\mu_1(\mathrm{d}z_1)\times\mu_2(\mathrm{d}z_2)\times\cdots\times\mu_l(\mathrm{d}z_l). \tag{10}$$

For average system (8) and (9), we consider the following assumption.

Assumption 4. The average system (8) and (9) has a solution on $[-D,+\infty)$.

Remark 3. By Assumption 1, we know that for any trajectory of the process $(Z(t), t\geqslant 0)$ and for any $X_0(t)\in\mathscr{C}_n$, system (6) and (7) has a unique solution up to a possible explosion time [33]. Assumption 2 implies that there is no finite explosion time for system (6) and (7), so that system (6) and (7) has a solution defined on the whole time interval $[-D,+\infty)$. In addition, according to Theorem 3.1 of [29], if system (6) and (7) satisfies the linear growth condition besides the locally Lipschitz condition, then it has a unique global solution in the almost sure sense. But in fact, owing to the approximation relationship of system (6) and (7) and its average system (8) and (9), the existence of the solution of system (6) and (7) can be guaranteed when the average system (8) and (9) has a solution on $[-D,+\infty)$. And the uniqueness of the solution of system (6) and (7) can be guaranteed by the locally Lipschitz condition in Assumption 1.

Lemma 1. Consider system (6) and (7) and system (8) and (9) under Assumptions 1–4. Then for any $T>0$,

$$\lim_{\epsilon_1\to 0}\sup_{-D\leqslant t\leqslant T}\left|X^{\epsilon_1}(t)-\bar{X}(t)\right|=0,\quad \text{a.s.} \tag{11}$$

Proof. See Appendix A.

Remark 4. In [29], the original system is a stochastic functional differential system that is assumed to satisfy both locally Lipschitz condition and the linear growth condition. Under such assumptions, Ref. [29] gave the approximation results between the solution of the original system and that of its average system in the sense of weak convergence. Here we focus on the delay-differential nonlinear locally Lipschitz system and give approximation results in the almost sure sense.

Next, we extend the finite-time approximation result in Lemma 1 to arbitrarily long time intervals.

Theorem 1. Consider system (6) and (7) and system (8) and (9) under Assumptions 1–4. Then for any $\delta>0$,

$$\lim_{\epsilon_1\to 0}\inf\{t\geqslant -D:|X^{\epsilon_1}(t)-\bar{X}(t)|>\delta\}=+\infty,\quad \text{a.s.} \tag{12}$$

Proof. The proof of this theorem follows from the proof of Theorem 1 in [34].

Now, we give the stability analysis of system (6) and (7) using the stability of averaged system (8) and (9) and Theorem 1. Here the stability concept of the system (8) and (9) refers to [35].

Theorem 2. Consider system (6) and (7) and system (8) and (9) under Assumptions 1–4. Then if the equilibrium solution $\bar{X}(t)\equiv 0$ of the average system (8) and (9) is exponentially stable, there exist constants $r>0$, $c>0$, $\nu>0$, such that, for any initial condition $X_0(t)\in\{\varphi\in\mathscr{C}_n:\|\varphi\|<r\}$ and any $\delta>0$, the solution of system (6) and (7) satisfies

$$\lim_{\epsilon_1\to 0}\inf\{t\geqslant -D:|X^{\epsilon_1}(t)|>c\big\|X_0(t)\big\|\exp\big\{-\nu t\big\}+\delta\}=+\infty,\quad \text{a.s.} \tag{13}$$

Proof. The proof of this theorem follows from the proof of Theorem 2 in [34].

Remark 5. If the equilibrium solution $\bar{X}(t)\equiv 0$ of the average system (8) and (9) is globally exponentially stable, then from Theorem 1, we can obtain that Eq. (13) holds for any initial condition $X_0(t)\in\mathscr{C}_n$.

4 Distributed source seeking and formation control

In this section, we consider designing a distributed stochastic source seeking algorithm to tune the velocity inputs of the vehicles based on the stochastic extremum seeking method and the leaderless formation control strategy. Since there exists a fixed time delay ($D>0$) in the process of information measurement, the vehicles can only obtain their historical measurements delayed by D time units. Specifically speaking, when $t>D$, the measurement of the scalar signal field measured by vehicle i, $i\in\mathcal{V}$ at time t is

$$f_i(t)=f(x_i(t-D)),$$

and the relative position measured at time t is

$$x_i(t-D)-x_j(t-D),\quad j\in\mathcal{N}_i.$$

When $0 \leqslant t \leqslant D$, vehicle i uses its measurement information at its initial position, namely

$$f_i(t) = f(x_i(0)), \tag{14}$$
$$x_i(t-D) - x_j(t-D) = x_i(0) - x_j(0), \quad j \in \mathcal{N}_i, \tag{15}$$

where $x_i(0)$ is the initial position of vehicle i, $f(x_i(0))$ is the signal measurement at the initial position of vehicle i, and $x_i(0) - x_j(0)$ is its initial relative position to the neighbor vehicle j.

During the stochastic extremum seeking algorithm design, vehicle i uses the following excitation signals for $i \in \mathcal{V}$:

$$\varepsilon_i \mathrm{d}\eta_{ij}(t) = -\eta_{ij}(t)\mathrm{d}t + \sqrt{\varepsilon_i} q_{ij} \mathrm{d}W_{ij}(t), \quad j \in \{1,2\}, \quad \forall t \geqslant 0, \tag{16}$$

where $q_{i1}, q_{i2} > 0$ are design parameters, and $0 < \varepsilon_i < \varepsilon_0$, $i \in \mathcal{V}$ are small parameters for fixed $\varepsilon_0 > 0$. For $j \in \{1,2\}$, $(W_{ij}(t), t \geqslant 0)$ is a standard one-dimensional Wiener processes defined on the complete probability space $(\Omega, \mathcal{F}, P)$ with the sample space Ω, σ-field $\mathcal{F}$, and probability measure P. We assume that $(W_{ij}(t), t \geqslant 0)$, $i \in \mathcal{V}$, $j \in \{1,2\}$ are mutually independent.

Moreover, we need to construct $M_i(t)$ and $N_i(t)$ such that $M_i(t)$ generates the gradient estimate $M_i(t)f_i(t)$ of the function f and $N_i(t)$ generates its Hessian matrix estimate $N_i(t)f_i(t)$. At this point, we choose $M_i(t)$ and $N_i(t)$ to satisfy

$$\begin{aligned} &\mathrm{Ave}\big\{M_i(t)\big\} = 0, \quad \mathrm{Ave}\big\{M_i(t)(\sin(\eta_i(t)))^{\mathrm{T}}\big\} = b_i^{-1}, \quad \mathrm{Ave}\big\{M_i(t)(\sin(\eta_i(t)))^{\mathrm{T}} b_i H b_i \sin(\eta_i(t))\big\} = 0, \\ &\mathrm{Ave}\big\{N_i(t)\big\} = 0, \quad \mathrm{Ave}\big\{N_i(t)(\sin(\eta_i(t)))^{\mathrm{T}}\big\} = 0, \quad \mathrm{Ave}\big\{N_i(t)(\sin(\eta_i(t)))^{\mathrm{T}} b_i H b_i \sin(\eta_i(t))\big\} = H. \end{aligned}$$

Since for $j, k \in \{1,2\}$,

$$\begin{aligned} \mathrm{Ave}\big\{\sin(\eta_{ij})\big\} &= \int_{\mathbb{R}} \sin(x)\mu_{ij}(\mathrm{d}x) = 0, \\ \mathrm{Ave}\big\{\sin(\eta_{ij})\sin(\eta_{ik})\big\} &= \int_{\mathbb{R}\times\mathbb{R}} \sin(x)\sin(y)\mu_{ij}(\mathrm{d}x) \times \mu_{ik}(\mathrm{d}y) \\ &= \begin{cases} \frac{1}{2}(1 - \exp\{-q_{ij}^2\}) \triangleq G_0(q_{ij}), & j = k, \\ 0, & j \neq k, \end{cases} \\ \mathrm{Ave}\big\{\sin(\eta_{ij})\sin^2(\eta_{ik})\big\} &= \int_{\mathbb{R}\times\mathbb{R}} \sin(x)\sin^2(y)\mu_{ij}(\mathrm{d}x) \times \mu_{ik}(\mathrm{d}y) = 0, \\ \mathrm{Ave}\big\{\sin(\eta_{ij}^2)\sin^2(\eta_{ik})\big\} &= \int_{\mathbb{R}\times\mathbb{R}} \sin^2(x)\sin^2(y)\mu_{ij}(\mathrm{d}x) \times \mu_{ik}(\mathrm{d}y) \\ &= \begin{cases} \frac{3}{8} - \frac{1}{2}\exp\{-q_{ij}^2\} + \frac{1}{8}\exp\{-4q_{ij}^2\} \triangleq G_1(q_{ij}), & j = k, \\ G_0(q_{ij})G_0(q_{ik}), & j \neq k, \end{cases} \end{aligned}$$

we choose

$$M_i(t) = \left[\frac{1}{b_{i1}G_0(q_{i1})}\sin(\eta_{i1}(t)), \frac{1}{b_{i2}G_0(q_{i2})}\sin(\eta_{i2}(t))\right]^{\mathrm{T}}, \tag{17}$$

$$N_i(t) = \begin{bmatrix} \frac{4(\sin^2(\eta_{i1}(t)) - G_0(q_{i1}))}{b_{i1}^2 G_0^2(\sqrt{2}q_{i1})} & \frac{\sin(\eta_{i1}(t))\sin(\eta_{i2}(t))}{b_{i1}b_{i2}G_0(q_{i1})G_0(q_{i2})} \\ \frac{\sin(\eta_{i1}(t))\sin(\eta_{i2}(t))}{b_{i1}b_{i2}G_0(q_{i1})G_0(q_{i2})} & \frac{4(\sin^2(\eta_{i2}(t)) - G_0(q_{i2}))}{b_{i2}^2 G_0^2(\sqrt{2}q_{i2})} \end{bmatrix}, \tag{18}$$

where $G_0^2(\sqrt{q_{ij}}) = 2(G_1(q_{ij}) - G_0^2(q_{ij}))$, and $b_{i1}, b_{i2} > 0$ are design parameters.

Then, for a predefined formation $h = (h_1^{\mathrm{T}}, \ldots, h_N^{\mathrm{T}})^{\mathrm{T}} \in \mathbb{R}^{2N}$, a block diagram of distributed source seeking and formation control for each vehicle is shown in Figure 1. Specifically, we employ the following algorithm to tune the velocity of vehicle i:

$$v_i(t) = k_1\xi_i(t) + b_i \frac{\mathrm{d}\sin\big(\eta_i(t+D)\big)}{\mathrm{d}t}, \tag{19}$$

$$\dot{\xi}_i(t) = k_1 \left\{ N_i(t)f_i(t)\xi_i(t) - k_2 \sum_{j\in\mathcal{N}_i} a_{ij}\big(\xi_i(t) - \xi_j(t)\big) \right\} + k_3 \Big\{ M_i(t)f_i(t) - N_i(t)f_i(t)\big(h_i - h^*\big)$$

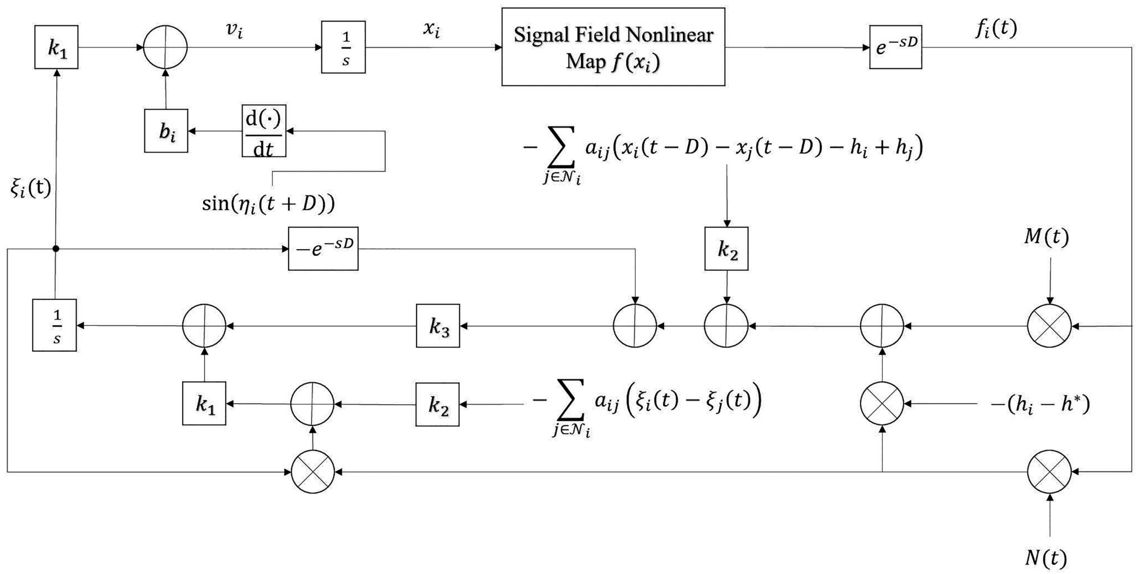

Figure 1 Block diagram of distributed source seeking and formation control for the ith vehicle.

$$- k_2 \sum_{j\in\mathcal{N}_i} a_{ij}\big(x_i(t-D) - x_j(t-D) - h_i + h_j\big) - \xi_i(t-D)\Bigg\},\tag{20}$$

where $\xi_i(\theta) = \varphi_i(\theta)$ if $\theta \in [-D, 0]$, $\varphi_i \in \mathscr{C}_2$, $k_1, k_2, k_3 > 0$ are design parameters, $b_i = \mathrm{diag}\{b_{i1}, b_{i2}\}$, and $\eta_i(t+D) = [\eta_{i1}(t+D), \eta_{i2}(t+D)]^{\mathrm{T}}$.

In contrast to the stochastic extremum seeking algorithm in [32], a one-stage sequential predictor from [25] is applied to compensate for the time delay $D > 0$ in the algorithm (19) and (20), where $\xi_i(t)$ is the state of the one-stage sequential predictor. Vehicle i can receive the current state $\xi_j(t)$ from its neighbor vehicle j in real time through the communication graph $\mathcal{G}$, and $\sum_{j\in\mathcal{N}_i} a_{ij}(\xi_i(t)-\xi_j(t))$ represents the information exchange between vehicle i and its neighbors. $M_i(t)f_i(t)$ is used to guide vehicle i toward the signal source, $-\sum_{j\in\mathcal{N}_i} a_{ij}(x_i(t-D) - x_j(t-D) - h_i + h_j)$ is used to allow the vehicles to achieve the formation h, and the compensated formation term $-N_i(t)f_i(t)(h_i - h^*)$ is used to allow the vehicles to keep this formation moving around the signal source, where $h_i - h^*$ represents the relative position between vehicle i and the mean center h^* of the formation h. As stated in [24, 26], we can advance (16) by D time units to generate the signal $\eta_{ij}(t+D)$ since $\eta_{ij}(t)$ is completely determined by (16) for $i \in \mathcal{V}$ and $j \in \{1, 2\}$.

Remark 6. Compared with the existing work about distributed source seeking with leaderless formation control strategy (e.g., [18, 21, 22]), the difference lies in two aspects. One is that real-time measurements without time delays are considered in [18, 21, 22], while we design the algorithm based on delayed measurements. The other is that the measurement information used to estimate the gradient of the scalar signal field is different. In our algorithm based on the stochastic extremum seeking method, each agent uses only its own signal measurements besides relative positions, while for the algorithms based on the (weighted) least squares method in [18, 21, 22], each agent also utilizes signal measurements of its neighbors besides its own signal measurements and relative positions.

We give the convergence results under the following assumption.

Assumption 5. The spatial distribution $f(x)$ of the signal field is a quadratic function, namely

$$f(x) = f^* + \frac{1}{2}(x - x^*)^{\mathrm{T}} H (x - x^*),\tag{21}$$

where f^* is the maximum and $H = H^{\mathrm{T}}$ is an unknown negative definite matrix.

Let $x(t) = [x_1^{\mathrm{T}}(t), \ldots, x_N^{\mathrm{T}}(t)]^{\mathrm{T}}$; then we have the following result.

Theorem 3. Consider the N velocity-actuated vehicles (1) navigated by the distributed stochastic source seeking algorithm (19) and (20) under Assumption 5 and the connected undirected graph $\mathcal{G}$. For a given constant $\gamma > 2$, the known delay $D > 0$, and a predefined formation $h = (h_1^{\mathrm{T}}, h_2^{\mathrm{T}}, \ldots, h_N^{\mathrm{T}})^{\mathrm{T}} \in \mathbb{R}^{2N}$, we choose $k_i > 0$, $i \in \{1,2,3\}$ satisfying

$$k_1\lambda_0 \neq \frac{\rho}{2}, \quad k_1\lambda_1 \neq \frac{\rho}{2}, \quad \sqrt{2\gamma}k_3 D < 1,$$

where $\rho = \min\{k_3(1-2\gamma k_3^2 D^2), \frac{\gamma-2}{2\gamma D}\} > 0$, $\lambda_0 = \lambda_{\min}(-((I_N \otimes H) - k_2(\mathcal{L}\otimes I_2)))$, and $\lambda_1 = \lambda_{\min}(-H)$.

Then there exist constants $0 < \nu_0 \leqslant (k_1\lambda_0 \wedge \frac{\rho}{2})$ and $0 < \nu_1 \leqslant (k_1\lambda_1 \wedge \frac{\rho}{2})$, such that for any initial conditions $x(0) \in \mathbb{R}^{2N}$ and $\varphi_i \in \mathscr{C}_2$, and any $\delta > 0$,

$$\lim_{\varepsilon_1 \to 0} \inf\left\{t \geqslant 0 : \left|x(t) - \mathbf{1}_N \otimes c(t) - h + \mathbf{1}_N \otimes h^*\right| > \mu_0 \exp\left\{-\nu_0 t\right\} + \delta + O(b)\right\} = +\infty, \quad \text{a.s.} \tag{22}$$

and

$$\lim_{\varepsilon_1 \to 0} \inf\left\{t \geqslant 0 : \left|c(t) - x^*\right| > \mu_1 \exp\left\{-\nu_1 t\right\} + \delta + O(b)\right\} = +\infty, \quad \text{a.s.}, \tag{23}$$

where μ_0 and μ_1 are defined as

$$\mu_0 = \left|x(0) - \mathbf{1}_N \otimes c(0) - h + \mathbf{1}_N \otimes h^*\right| + \frac{k_1}{\left|k_1\lambda_0 - \frac{\rho}{2}\right|}\gamma_0, \tag{24}$$

$$\mu_1 = \left|c(0) - x^*\right| + \frac{k_1}{\sqrt{N}\left|k_1\lambda_1 - \frac{\rho}{2}\right|}\gamma_0, \tag{25}$$

with $\gamma_0 = \left|((I_N \otimes H) - k_2(\mathcal{L}\otimes I_2))(x(0) - \mathbf{1}_N \otimes x^* - h + \mathbf{1}_N \otimes h^*)\right| + \|\varphi\|$, $\varphi = [\varphi_1^{\mathrm{T}}, \ldots, \varphi_N^{\mathrm{T}}]^{\mathrm{T}}$, $c(0) = \frac{1}{N}\sum_{i=1}^N x_i(0)$, $h^* = \frac{1}{N}\sum_{i=1}^N h_i$, and $b = \sqrt{\sum_{i=1}^N \left(b_{i1}^2 + b_{i2}^2\right)}$.

Proof. See Appendix C.

Remark 7. As shown in (22), the vehicles can achieve a formation h almost surely at the convergence rate ν_0 as $\varepsilon_1 \to 0$, and Eq. (23) shows that the average position of vehicles converges to a small neighborhood of the signal source almost surely at the convergence rate ν_1 as $\varepsilon_1 \to 0$. By (22) and (23), we obtain that $\lim_{\varepsilon_1\to 0} \inf\{t \geqslant 0 : |x(t) - \mathbf{1}_N \otimes x^* - h + \mathbf{1}_N \otimes h^*| > (\mu_0 \vee \mu_1)\exp\{-(\nu_0 \wedge \nu_1)t\} + \delta + O(b)\} = +\infty$, a.s.. This means that the vehicles eventually keep this formation moving around the signal source with some offsets $(h - \mathbf{1}_N \otimes h^*)$ from the source, and $h - \mathbf{1}_N \otimes h^*$ should not be too large to ensure that the vehicles can get closer to the source.

Remark 8. From Theorem 3, we know that an arbitrarily long delay can be compensated by choosing the parameter k_3 satisfying $\sqrt{2\gamma}k_3 D < 1$. It is clear that k_3 is inversely proportional to the time delay, so the parameter k_3 becomes smaller as the time delay becomes longer. Moreover, we know that $\nu_0 \vee \nu_1$ is less than $\frac{\rho}{2}$ with $0 < \rho \leqslant \frac{2}{3}k_3$, so ν_0 and ν_1 become smaller as the parameter k_3 becomes smaller. Therefore, the longer the time delay is, the slower the convergence rate will become. Additionally, in view of ν_0 and ν_1, we obtain that if $0 < k_1\lambda_i < \frac{\rho}{2}$, $i \in \{1,2\}$ hold, then the larger the parameter k_1 is, the faster the convergence rate will be.

Remark 9. From (22) and (23), we can obtain that a larger b_{ij}, $i \in \mathcal{V}$, $j \in \{1,2\}$ may lead to an increase in convergence errors. From (24) and (25), it can be seen that μ_i is positively correlated with $\frac{k_1}{|k_1\lambda_i - \frac{\rho}{2}|}$ for $i \in \{0,1\}$. This means that when the initial positions of the vehicles are given, if the parameter k_1 is sufficiently small, then μ_0 tends to $|x(0) - \mathbf{1}_N \otimes c(0) - h + \mathbf{1}_N \otimes h^*|$ and μ_1 tends to $|c(0) - x^*|$ according to (24) and (25). On this basis, if the initial formation of the vehicles is the same as the predefined formation, their initial average position is far away from the signal source, and k_1 is sufficiently smaller, then the vehicles will move slowly in this formation toward the signal source according to (22) and (23).

Remark 10. Under the assumption that the function $f(x)$ is quadratic, Theorem 3 gives the global exponential convergence result. For any second-order continuous differentiable function $f(x)$, if it has an extremum at the point x^* and a nonzero Hessian matrix, we apply the Taylor expansion to $f(x)$ around x^* up to second order and then obtain a quadratic function similar to (21). At this point, we can obtain the local exponential convergence result by Theorem 3.

5 Numerical simulation

In this section, we present numerical simulations to show the effectiveness of the proposed algorithm. In Subsection 5.1, we show that the algorithm allows vehicles to achieve a specific formation in the source

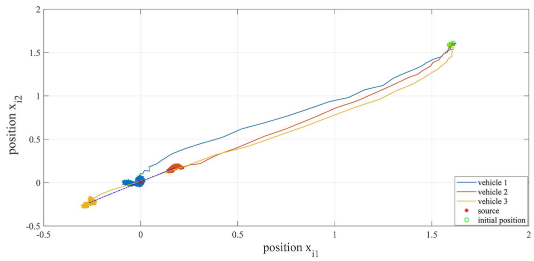

Figure 2 Trajectories of the three vehicles during the source seeking process.

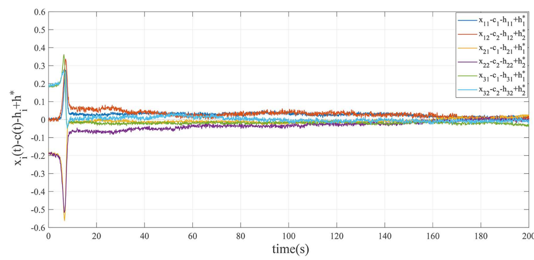

Figure 3 Offsets of the three vehicles from their average positions.

seeking process and eventually keep this formation moving around the signal source. In Subsection 5.2, we show the effect of design parameters and the time delay on the performance of the proposed algorithm. During all the simulations, the spatial distribution of the scalar signal field is assumed to be

$$f(x) = 4 - \frac{1}{2}(x - x^*)^{\mathrm{T}} \begin{bmatrix} -2 & 0 \\ 0 & -2 \end{bmatrix} (x - x^*),$$

where $x^* = (0,0)^{\mathrm{T}}$ denotes the signal source location, and the model of each vehicle is described by (1).

5.1 Cooperative source seeking and formation control

In this subsection, we illustrate the effectiveness of the proposed algorithm by considering a straight line formation of three vehicles (Figures 2–5) and a square formation of four vehicles (Figures 6–9) when the time delay of the information measurement process is $D = 1$ s. In Figures 2–4, the initial positions of the vehicles are $x_1(0) = (1.6, 1.6)^{\mathrm{T}}$, $x_2(0) = (1.61, 1.61)^{\mathrm{T}}$, $x_3(0) = (1.59, 1.59)^{\mathrm{T}}$, and the parameters are chosen as $k_1 = 0.00000103$, $k_3 = 0.0001$, $b_{11} = 0.00211$, $b_{12} = 0.003$, $b_{21} = 0.001662$, $b_{22} = 0.001704$, $b_{31} = 0.001585$, $b_{32} = 0.002190$, $k_2 = 0.35$. In Figures 6–8, the initial positions of the vehicles are $x_1(0) = (10, 10)^{\mathrm{T}}$, $x_2(0) = (-8, -8)^{\mathrm{T}}$, $x_3(0) = (-8, 10)^{\mathrm{T}}$, $x_4(0) = (10, -8)^{\mathrm{T}}$, and the parameters are chosen as $k_1 = 0.00002$, $k_3 = 0.33$, $\varepsilon = 0.001$, $q_{x1} = q_{x2} = q_{x3} = q_{x4} = 12.6491$, $q_{y1} = 15.8114$, $q_{y2} = q_{y3} = q_{y4} = 13.2816$, $b_{11} = 0.252$, $b_{12} = 0.251$, $b_{21} = 0.283$, $b_{22} = 0.276$, $b_{31} = 0.285$, $b_{32} = 0.255$, $b_{41} = 0.262$, $b_{42} = 0.283$, $k_2 = 0.001$.

Figures 2 and 3 show that the vehicles stay in this formation once they achieve a straight line formation defined by $h_1 = (0, 0)^{\mathrm{T}}$, $h_2 = (0.2, 0.2)^{\mathrm{T}}$, $h_3 = (-0.2, -0.2)^{\mathrm{T}}$, when they communicate via the graph shown in Figure 5. Figures 6 and 7 show that the vehicles stay in this formation once they achieve a square formation defined by $h_1 = (1.5, 1.5)^{\mathrm{T}}$, $h_2 = (-1.5, -1.5)^{\mathrm{T}}$, $h_3 = (-1.5, 1.5)^{\mathrm{T}}$, $h_4 = (1.5, -1.5)^{\mathrm{T}}$, when they communicate via the graph shown in Figure 9. Figures 4 and 8 depict that the average position of the vehicles converges to a small neighborhood of the signal source. By Figures 3 and 4, or by Figures 7 and 8, it can be seen that the vehicles achieve a formation while seeking the signal source and ultimately keep this formation moving around the signal source. From Figures 2 and 6, it can be seen that the application of the formation control can avoid the gathering of vehicles near the signal source, thus effectively avoiding collisions when the vehicles move around the signal source.

5.2 Effects of design parameters and time delay

In this subsection, we consider four vehicles and the communication graph shown in Figure 9 to show the effect of design parameters and the time delay on the performance of the proposed algorithm. In comparison to the stochastic extremum seeking algorithm in [32], the new parameters k_i, $i \in \{1, 2, 3\}$ are added in the algorithm (19) and (20), so we mainly focus on the effect of parameters k_i, $i \in \{1, 2, 3\}$ and time delay D on the performance of this algorithm, when the other parameters are taken as in Figures 6–8.

Compared with Figures 7 and 8, Figures 10 and 11 show that the convergence rate will be slower when we choose a smaller k_1 satisfying $0 < k_1\lambda_i < \frac{\rho}{2}$, $i \in \{0, 1\}$.

From Theorem 3, we know that k_3 affects the delay compensation rate, and the length of the delay D in turn affects the value of k_3. We therefore analyze the effect of both k_3 and D on the performance of the algorithm. Compared with Figures 12 and 13, Figures 14 and 15 depict that the convergence rate

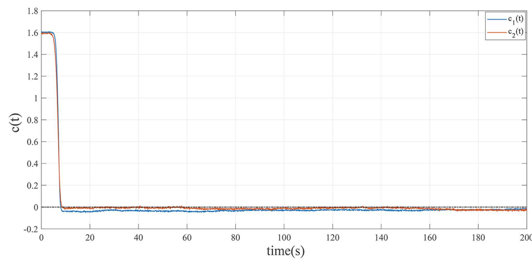

Figure 4 Trajectories of the average positions of three vehicles.

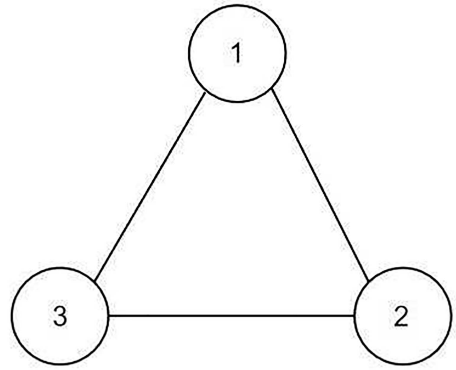

Figure 5 Communication graph between three vehicles.

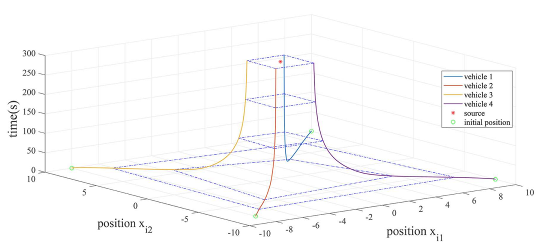

Figure 6 Trajectories of four vehicles. And the blue dotted lines from bottom to top are the formations of the vehicles at the 5th, 10th, 100th, 200th, and 300th second.

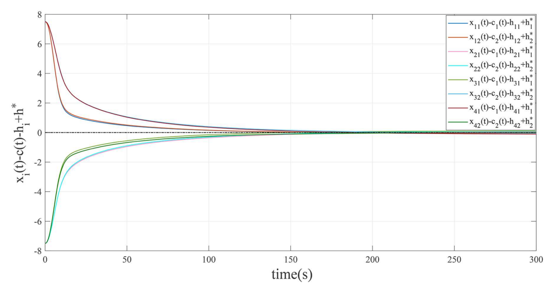

Figure 7 Offsets of the four vehicles from their average positions.

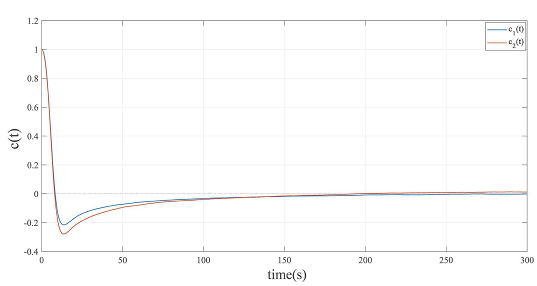

Figure 8 Trajectories of the average positions of four vehicles.

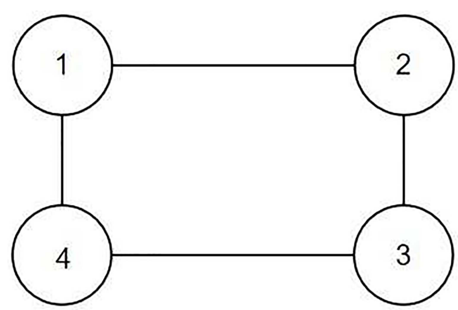

Figure 9 Communication graph between four vehicles.

will be slower when the time delay D becomes longer. Compared with Figures 7 and 8, Figures 12 and 13 show that changing the value of k_3 causes the value of k_1 to become smaller, and the convergence rate becomes slower.

The value of k_2 has an effect on the formation realization. From Figures 2 and 6, a larger k_2 is required when the vehicles are located in the same direction of the signal source, while a slightly smaller k_2 is required when the vehicles are located in different directions of the signal source. Figures 16 and 17 show that if the relative positions of the vehicles at the initial moment coincide with those in the predefined formation and a smaller k_1 as well as a larger k_2 are chosen, then vehicles maintain this formation without collision during the source seeking process. Figure 16 depicts a square formation and Figure 17 depicts a rhombic formation.

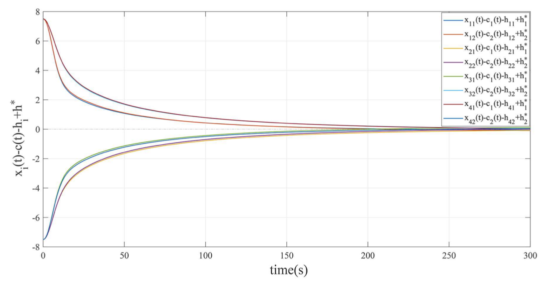

Figure 10 Trajectories of the four vehicles under $k_1 = 0.000018$ and $D = 1$ s.

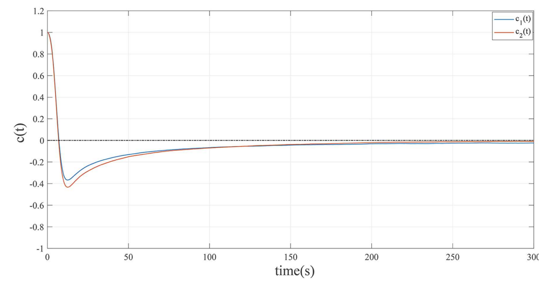

Figure 11 Offsets of the four vehicles from their average positions under $k_1 = 0.000018$ and $D = 1$ s.

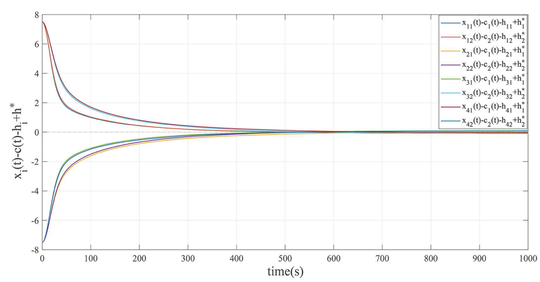

Figure 12 Trajectories of the four vehicles under $k_1 = 0.0000066$, $k_3 = 0.1245$, and $D = 1$ s.

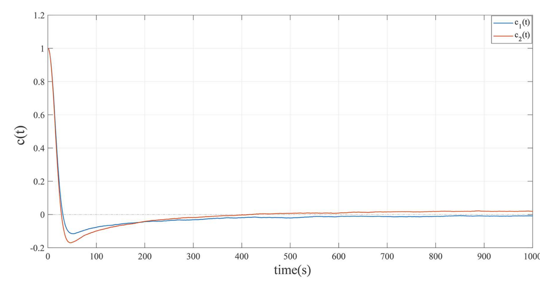

Figure 13 Offsets of the four vehicles from their average positions under $k_1 = 0.0000066$, $k_3 = 0.1245$, and $D = 1$ s.

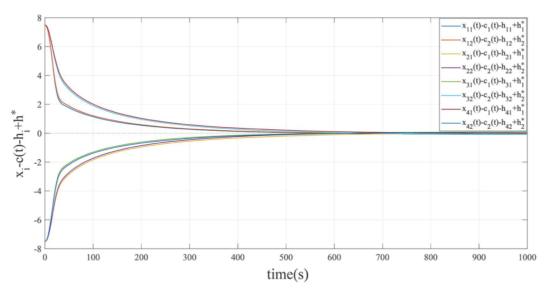

Figure 14 Trajectories of the four vehicles under $k_1 = 0.0000066$, $k_3 = 0.1245$, and $D = 4$ s.

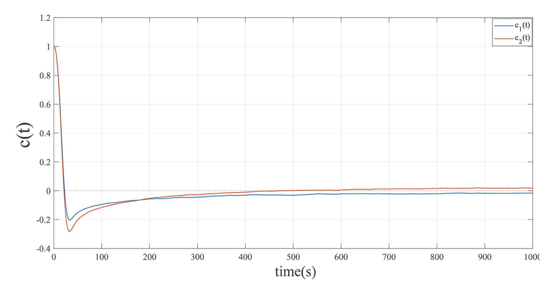

Figure 15 Offsets of the four vehicles from their average positions under $k_1 = 0.0000066$, $k_3 = 0.1245$, and $D = 4$ s.

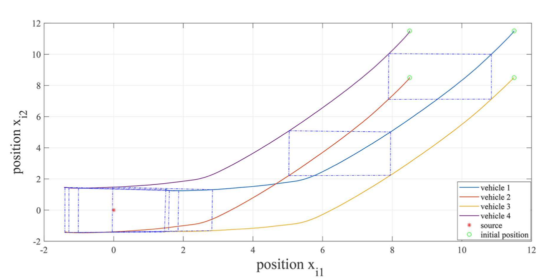

Figure 16 Trajectories of the four vehicles under $k_2 = 15$, $D = 1$ s, and $h_i = 1.5(\cos(\frac{2i\pi}{3}), \sin(\frac{2i\pi}{3}))^{\mathrm{T}}$, $i \in \{1,2,3,4\}$. The blue dotted lines from top to bottom are the formations of the four vehicles at the 5th, 10th, 100th, 200th, 300th, and 1000th second.

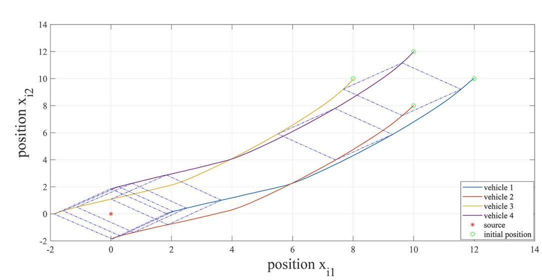

Figure 17 Trajectories of the four vehicles under $k_2 = 15$, $D = 1$ s and $h_i = 2(\sin(\frac{i\pi}{2}), \cos(\frac{i\pi}{2}))^{\mathrm{T}}$, $i \in \{1,2,3,4\}$. The blue dotted lines from top to bottom are the formations of the four vehicles at the 5th, 10th, 100th, 200th, 300th, and 1000th second.

6 Concluding remarks

To analyze the convergence of the stochastic extremum seeking algorithm based on time-delay measurements, we developed stochastic averaging theorems for a class of locally Lipschitz nonlinear time-delay systems with stochastic perturbations. Based on the stochastic extremum seeking method and the leaderless formation control strategy, we designed a distributed stochastic source seeking algorithm based on time-delay measurements to navigate multiple vehicles toward an unknown source while achieving and maintaining a predefined formation. Using the developed stochastic averaging theorems, we proved that the average position of the vehicles exponentially converged to a small neighborhood of the source in the almost sure sense, while a predefined formation was achieved and maintained.

The main limitation of this work is that the measurement delay is assumed to be a known constant and the communication topology is assumed to be fixed in order to obtain the rigorous analysis of convergence. In our next work, we will consider more practical types of time delay (e.g., time-varying, unknown) and more general communication topology.

Acknowledgements This work was supported by National Natural Science Foundation of China (Grant No. 62473272) and Natural Science Foundation of Sichuan Province, China (Grant No. 2024NSFSC0437).

References

1 Atanasov N A, Ny J L, Pappas G J. Distributed algorithms for stochastic source seeking with mobile robot networks. J Dynamic Syst Meas Control, 2015, 137: 031011
2 Sahal M, Hidayat Z, Alkaff A. Comparison of gradient estimation in cooperative multi-agent source seeking. J Adv Res Electr Eng, 2017, 1: 39–43
3 Li Z, You K, Song S. Cooperative source seeking via networked multi-vehicle systems. Automatica, 2020, 115: 108853
4 Yang L Y, Liu S J, Zhang P P. Stochastic time-varying extremum seeking and its applications. Automatica, 2023, 151: 110923
5 Ren W, Atkins E. Distributed multi-vehicle coordinated control via local information exchange. Intl J Robust Nonlinear, 2007, 17: 1002–1033
6 Oh K K, Ahn H S. Formation control of mobile agents based on inter-agent distance dynamics. Automatica, 2011, 47: 2306–2312
7 Li C, Qu Z, Weitnauer M A. Distributed extremum seeking and formation control for nonholonomic mobile network. Syst Control Lett, 2015, 75: 27–34
8 Nuno E, Loria A, Panteley E. Leaderless consensus formation control of cooperative multi-agent vehicles without velocity measurements. IEEE Control Syst Lett, 2021, 6: 902–907
9 Binetti P, Ariyur K B, Krstic M, et al. Formation flight optimization using extremum seeking feedback. J Guid Control Dyn, 2003, 26: 132–142
10 Shen D B, Sun Z D, Sun W J. Leader-follower formation control without leader's velocity information. Sci China Inf Sci, 2014, 57: 092202
11 Wang N, Zhang T W, Xu J Q. Formation control for networked spacecraft in deep space: with or without communication delays and with switching topology. Sci China Inf Sci, 2011, 54: 469–481
12 He X D, Geng Z Y. Leader-follower formation control of underactuated surface vessels. Sci China Inf Sci, 2022, 65: 209201
13 Yin T, Gu Z, Park J H. Event-based intermittent formation control of multi-UAV systems under deception attacks. IEEE Trans Neural Netw Learn Syst, 2024, 35: 8336–8347
14 Li W H, Zhang H G, Zhang J, et al. Fully distributed dynamic event-triggered formation-containment tracking for multiagent systems with multiple types of disturbances. Sci China Inf Sci, 2024, 67: 112203
15 Biyik E, Arcak M. Gradient climbing in formation via extremum seeking and passivity-based coordination rules. Asian J Control, 2008, 10: 201–211
16 Paliotta C, Belleter D J W, Pettersen K Y. Adaptive source seeking with leader-follower formation control. IFAC-PapersOnLine, 2015, 48: 285–290
17 Skobeleva A, Fidan B, Ugrinovskii V, et al. Planar cooperative extremum seeking with guaranteed convergence using a three-robot formation. In: Proceedings of IEEE Conference on Decision and Control, 2018. 1305–1310
18 Rosero E, Werner H. Cooperative source seeking via gradient estimation and formation control (part 2). In: Proceedings of UKACC International Conference on Control, 2014. 634–639
19 Briñón-Arranz L, Schenato L, Seuret A. Distributed source seeking via a circular formation of agents under communication constraints. IEEE Trans Control Netw Syst, 2016, 3: 104–115
20 Briñón-Arranz L, Renzaglia A, Schenato L. Multirobot symmetric formations for gradient and hessian estimation with application to source seeking. IEEE Trans Robot, 2019, 35: 782–789
21 Barogh S A, Werner H. Cooperative source seeking with distance-based formation control and single-integrator agents. IFAC-PapersOnLine, 2017, 50: 7911–7916
22 Barogh S A, Werner H. Cooperative source seeking with distance-based formation control and non-holonomic agents. IFAC-PapersOnLine, 2017, 50: 7917–7922
23 Oliveira T R, Krstic M, Tsubakino D. Extremum seeking for static maps with delays. IEEE Trans Automat Contr, 2016, 62: 1911–1926
24 Rušiti D, Oliveira T R, Mills G, et al. Deterministic and stochastic Newton-based extremum seeking for higher derivatives of unknown maps with delays. Eur J Control, 2018, 41: 72–83
25 Malisoff M, Krstic M. Multivariable extremum seeking with distinct delays using a one-stage sequential predictor. Automatica, 2021, 129: 109462
26 Rusiti D, Evangelisti G, Oliveira T R, et al. Stochastic extremum seeking for dynamic maps with delays. IEEE Control Syst Lett, 2019, 3: 61–66
27 Katafygiotis L, Tsarkov Y. Averaging and stability of quasilinear functional differential equations with Markov parameters. Int J Stoch Anal, 1999, 12: 1–15
28 White B S. Some limit theorems for stochastic delay-differential equations. Comm Pure Appl Math, 1976, 29: 113–141
29 Wu F, Yin G. Fast-slow-coupled stochastic functional differential equations. J Differ Equ, 2022, 323: 1–37
30 Fax J A, Murray R M. Information flow and cooperative control of vehicle formations. IEEE Trans Automat Contr, 2004, 49: 1465–1476
31 Krstić M. Delay Compensation for Nonlinear, Adaptive, and PDE Systems. Berlin: Springer, 2009
32 Liu S J, Krstić M. Stochastic Averaging and Stochastic Extremum Seeking. Berlin: Springer, 2012
33 Yuan C, Mao X. Robust stability and controllability of stochastic differential delay equations with Markovian switching. Automatica, 2004, 40: 343–354
34 Liu S J, Krstic M. Stochastic averaging in continuous time and its applications to extremum seeking. IEEE Trans Automat Contr, 2010, 55: 2235–2250

35 Driver R D. Existence and stability of solutions of a delay-differential system. Arch Rational Mech Anal, 1962, 10: 401–426

Appendix A Proof of Lemma 1

Proof. The proof idea comes from [34]. Since $X^{\epsilon_1}(t) = \bar{X}(t) = X_0(t)$ if $t \in [-D, 0]$, we only analyze the approximation between the solution of system (6) and (7) and that of system (8) and (9) for $t > 0$.

By Assumption 1 and (10), it is not hard to verify that $\bar{f}(\cdot,\cdot)$ is locally Lipschitz. Then for each given initial condition $X_0(t) \in \mathscr{C}_n$, there exists a constant $\tau_a > 0$, such that system (8) and (9) has a unique continuous solution on $[-D, \tau_a]$[1]. Assumption 4 means that the system (8) and (9) has a unique continuous solution on $[-D, +\infty)$.

For a fixed $T > 0$, $[-D, T]$ is a compact set. Since $(\bar{X}(t), t \geqslant -D)$ is a deterministic continuous function, there exists a constant $M' < +\infty$ such that

$$M' = \sup_{-D\leqslant t\leqslant T} \left|\bar{X}(t)\right|. \tag{A1}$$

Let $M = M' + 1$. For any $\epsilon_1 \in (0, \epsilon_0)$, define a stopping time τ_{ϵ_1} as

$$\tau_{\epsilon_1} = \inf\{t \geqslant -D : |X^{\epsilon_1}(t)| > M\},$$

where $\inf \emptyset = +\infty$. By (A1), we know that $|X^{\epsilon_1}(t)| = |\bar{X}(t)| = |X_0(t)| \leqslant M' < M$ if $t \in [-D, 0]$.

Based on Assumption 2, the sample path of $(X^{\epsilon_1}(t), t \geqslant -D)$ is continuous, so we have $0 < \tau_{\varepsilon_1} \leqslant +\infty$, and if $\tau_{\epsilon_1} < +\infty$, then

$$\left|X^{\epsilon_1}(\tau_{\epsilon_1})\right| = M. \tag{A2}$$

For any $0 \leqslant s \leqslant \tau_{\epsilon_1} \wedge T$, $|X^{\epsilon_1}(s)| \vee |X^{\epsilon_1}(s-D)| \vee |\bar{X}(s)| \vee |\bar{X}(s-D)| \leqslant M$. In combination with Assumption 1, there exists a constant $L_M > 0$ such that

$$\begin{aligned}&\left|f\big(X^{\epsilon_1}(s), X^{\epsilon_1}(s-D), Z(s/\epsilon_1)\big) - f\big(\bar{X}(s), \bar{X}(s-D), Z(s/\epsilon_1)\big)\right| \\ &\leqslant L_M\Big(\left|X^{\epsilon_1}(s) - \bar{X}(s)\right| + \left|X^{\epsilon_1}(s-D) - \bar{X}(s-D)\right|\Big).\end{aligned} \tag{A3}$$

Since for any $0 \leqslant t \leqslant D$,

$$\int_0^t \left|X^{\epsilon_1}(s-D) - \bar{X}(s-D)\right| \mathrm{d}s = \int_{-D}^{t-D} \left|X^{\epsilon_1}(s) - \bar{X}(s)\right| \mathrm{d}s = 0,$$

and for any $t > D$,

$$\int_0^t \left|X^{\epsilon_1}(s-D) - \bar{X}(s-D)\right| \mathrm{d}s = \int_{-D}^{0} \left|X^{\epsilon_1}(s) - \bar{X}(s)\right| \mathrm{d}s + \int_0^{t-D} \left|X^{\epsilon_1}(s) - \bar{X}(s)\right| \mathrm{d}s \leqslant \int_0^t \left|X^{\epsilon_1}(s) - \bar{X}(s)\right| \mathrm{d}s,$$

then if $0 \leqslant t \leqslant \tau_{\epsilon_1} \wedge T$, we have

$$\begin{aligned}\left|X^{\epsilon_1}(t) - \bar{X}(t)\right| &\leqslant \int_0^t L_M\Big(\left|X^{\epsilon_1}(s) - \bar{X}(s)\right| + \left|X^{\epsilon_1}(s-D) - \bar{X}(s-D)\right|\Big)\mathrm{d}s \\ &\quad + \left|\int_0^t \Big[f\big(\bar{X}(s), \bar{X}(s-D), Z(s/\epsilon_1)\big) - \bar{f}\big(\bar{X}(s), \bar{X}(s-D)\big)\Big]\mathrm{d}s\right| \\ &\leqslant 2L_M \int_0^t \left|X^{\epsilon_1}(s) - \bar{X}(s)\right| \mathrm{d}s + \left|\int_0^t \Big[f\big(\bar{X}(s), \bar{X}(s-D), Z(s/\epsilon_1)\big) - \bar{f}\big(\bar{X}(s), \bar{X}(s-D)\big)\Big]\mathrm{d}s\right|.\end{aligned} \tag{A4}$$

Let

$$\begin{aligned}\Delta^{\epsilon_1}(t) &= \left|X^{\epsilon_1}(t) - \bar{X}(t)\right|, \\ \alpha(\epsilon_1) &= \sup_{0\leqslant t\leqslant T}\left|\int_0^t \Big[f\big(\bar{X}(s), \bar{X}(s-D), Z(s/\epsilon_1)\big) - \bar{f}\big(\bar{X}(s), \bar{X}(s-D)\big)\Big]\mathrm{d}s\right|.\end{aligned}$$

Then, Eq. (A4) can be rewritten as

$$\Delta^{\epsilon_1}(t) \leqslant 2L_M \int_0^t \Delta^{\epsilon_1}(s)\mathrm{d}s + \alpha(\epsilon_1), \quad \forall 0 \leqslant t \leqslant \tau_{\epsilon_1} \wedge T.$$

Thus by Gronwall's inequality, we have

$$\Delta^{\epsilon_1}(t) \leqslant \alpha(\epsilon_1)\mathrm{e}^{\int_0^t 2L_M \mathrm{d}s} = \alpha(\epsilon_1)\mathrm{e}^{2L_M t}, \quad \forall 0 \leqslant t \leqslant \tau_{\epsilon_1} \wedge T.$$

1) Hale J K, Lunel S M V. Introduction to Functional Differential Equations. Berlin: Springer, 2013.

That is,

$$\sup_{0\leqslant t\leqslant \tau_{\epsilon_1}\wedge T} \Delta^{\epsilon_1}(t) \leqslant \alpha(\epsilon_1)\mathrm{e}^{2L_M(\tau_{\epsilon_1}\wedge T)} \leqslant \alpha(\epsilon_1)\mathrm{e}^{2L_M T}. \tag{A5}$$

Similar to [34], we have

$$\lim_{\epsilon_1\to 0} \alpha(\epsilon_1) = 0, \quad \text{a.s.} \tag{A6}$$

For the convenience of readers, the detailed proof of (A6) is given in Appendix B. Then by (A5) and (A6), we have

$$\limsup_{\epsilon_1\to 0} \sup_{0\leqslant t\leqslant \tau_{\epsilon_1}\wedge T} \left|X^{\epsilon_1}(t) - \bar{X}(t)\right| = 0, \quad \text{a.s.} \tag{A7}$$

By (A1) and (A7), we have

$$\begin{aligned}\limsup_{\epsilon_1\to 0} \sup_{0\leqslant t\leqslant \tau_{\epsilon_1}\wedge T} \left|X^{\epsilon_1}(t)\right| &\leqslant \limsup_{\epsilon_1\to 0}\Big[\sup_{0\leqslant t\leqslant \tau_{\epsilon_1}\wedge T} \left|X^{\epsilon_1}(t) - \bar{X}(t)\right| + \sup_{0\leqslant t\leqslant \tau_{\epsilon_1}\wedge T}\left|\bar{X}(t)\right|\Big]\\ &\leqslant \limsup_{\epsilon_1\to 0} \sup_{0\leqslant t\leqslant \tau_{\epsilon_1}\wedge T} \left|X^{\epsilon_1}(t) - \bar{X}(t)\right| + M'\\ &< M, \quad \text{a.s.}\end{aligned} \tag{A8}$$

From (A2) and (A8), for almost all $\omega\in\Omega$, there exists a constant $\epsilon^*(\omega) > 0$ such that if $0 < \epsilon_1 < \epsilon^*(\omega)$, we have

$$\tau_{\epsilon_1}(\omega) > T. \tag{A9}$$

Thus using (A7) and (A9), we have

$$\limsup_{\epsilon_1\to 0} \sup_{0\leqslant t\leqslant T} \left|X^{\epsilon_1}(t) - \bar{X}(t)\right| = 0, \quad \text{a.s.}$$

The proof is completed.

Appendix B Proof of (A6)

Proof. For a positive integer n, we set $\kappa = \frac{D}{n}$ and divide the interval $[-D, +\infty)$ into equidistant cells $[i\kappa, (i+1)\kappa)$ with integer $i \geqslant -n$. For $s \in \big[i\kappa, (i+1)\kappa\big)$, we define $\bar{X}^n(s)$ as

$$\bar{X}^n(s) = \bar{X}(i\kappa). \tag{B1}$$

Obviously, for any $i \geqslant 0$, when $s \in \big[i\kappa, (i+1)\kappa\big)$, we know $s - D = s - n\kappa \in \big[(i-n)\kappa, (i-n+1)\kappa\big)$. Based on the definition of $\bar{X}^n(s)$, we have $\bar{X}^n(s-D) = \bar{X}((i-n)\kappa) = \bar{X}(i\kappa - D)$. Meanwhile, we know

$$\sup_{-D\leqslant s\leqslant T} \left|\bar{X}^n(s)\right| \leqslant \sup_{-D\leqslant s\leqslant T} \left|\bar{X}(s)\right| = M' < M, \tag{B2}$$

where M, M' are defined in Appendix A. By Assumption 1 and (10), we get that there exists a constant $\tilde{L}_M > 0$ such that for all $x_1 \vee x_2 \vee \check{x}_1 \vee \check{x}_2 \leqslant M$ and $z \in S_{Y_1} \times S_{Y_2} \times \cdots \times S_{Y_l}$,

$$\begin{aligned}\left|f\big(x_1, x_2, z\big) - f\big(\check{x}_1, \check{x}_2, z\big)\right| &\leqslant \tilde{L}_M\big(|x_1 - \check{x}_1| + |x_2 - \check{x}_2|\big),\\ \left|\bar{f}(x_1, x_2) - \bar{f}(\check{x}_1, \check{x}_2)\right| &\leqslant \tilde{L}_M\big(|x_1 - \check{x}_1| + |x_2 - \check{x}_2|\big).\end{aligned}$$

Then, we have

$$\begin{aligned}&\sup_{0\leqslant t\leqslant T}\left|\int_0^t \Big[f\big(\bar{X}(s), \bar{X}(s-D), Z(s/\epsilon_1)\big) - \bar{f}\big(\bar{X}(s), \bar{X}(s-D)\big)\Big]\mathrm{d}s\right|\\ &\leqslant \sup_{0\leqslant t\leqslant T}\int_0^t \left|f\big(\bar{X}(s), \bar{X}(s-D), Z(s/\epsilon_1)\big) - f\big(\bar{X}^n(s), \bar{X}^n(s-D), Z(s/\epsilon_1)\big)\right|\mathrm{d}s\\ &\quad + \sup_{0\leqslant t\leqslant T}\left|\int_0^t f\big(\bar{X}^n(s), \bar{X}^n(s-D), Z(s/\epsilon_1)\big) - \bar{f}\big(\bar{X}^n(s), \bar{X}^n(s-D)\big)\mathrm{d}s\right|\\ &\quad + \sup_{0\leqslant t\leqslant T}\int_0^t \left|\bar{f}\big(\bar{X}^n(s), \bar{X}^n(s-D)\big) - \bar{f}\big(\bar{X}(s), \bar{X}(s-D)\big)\right|\mathrm{d}s\\ &\leqslant 2\tilde{L}_M \sup_{0\leqslant t\leqslant T}\int_0^t \Big(\left|\bar{X}(s) - \bar{X}^n(s)\right| + \left|\bar{X}(s-D) - \bar{X}^n(s-D)\right|\Big)\,\mathrm{d}s\end{aligned}$$

$$+\sup_{0\leqslant t\leqslant T}\left|\int_0^t\left[f(\bar{X}^n(s),\bar{X}^n(s-D),Z(s/\epsilon_1))-\bar{f}(\bar{X}^n(s),\bar{X}^n(s-D))\right]\mathrm{d}s\right|. \tag{B3}$$

For the second term on the right-hand side of the inequality (B3), we have

$$\begin{aligned}
&\sup_{0\leqslant t\leqslant T}\left|\int_0^t\left[f(\bar{X}^n(s),\bar{X}^n(s-D),Z(s/\epsilon_1))-\bar{f}(\bar{X}^n(s),\bar{X}^n(s-D))\right]\mathrm{d}s\right|\\
&=\sup_{0\leqslant t\leqslant T}\left|\sum_{i=0}^{\lfloor t/\kappa\rfloor}\int_{i\kappa\wedge t}^{(i+1)\kappa\wedge t}\left[f(\bar{X}^n(s),\bar{X}^n(s-D),Z(s/\epsilon_1))-\bar{f}(\bar{X}^n(s),\bar{X}^n(s-D))\right]\mathrm{d}s\right|\\
&=\sup_{0\leqslant t\leqslant T}\left|\sum_{i=0}^{\lfloor t/\kappa\rfloor}\int_{i\kappa\wedge t}^{(i+1)\kappa\wedge t}\left[f(\bar{X}(i\kappa),\bar{X}(i\kappa-D),Z(s/\epsilon_1))-\bar{f}(\bar{X}(i\kappa),\bar{X}(i\kappa-D))\right]\mathrm{d}s\right|\\
&\leqslant\sup_{0\leqslant t\leqslant T}\sum_{i=0}^{\lfloor t/\kappa\rfloor}\left|\int_{i\kappa\wedge t}^{(i+1)\kappa\wedge t}\left[f(\bar{X}(i\kappa),\bar{X}(i\kappa-D),Z(s/\epsilon_1))-\bar{f}(\bar{X}(i\kappa),\bar{X}(i\kappa-D))\right]\mathrm{d}s\right|,
\end{aligned} \tag{B4}$$

where $\lfloor \frac{t}{\kappa}\rfloor$ is the largest integer not greater than $\frac{t}{\kappa}$. For fixed n and $i\in\{0,\ldots,\lfloor\frac{t}{\kappa}\rfloor\}$,

$$\begin{aligned}
&\sup_{0\leqslant t\leqslant T}\left|\int_{i\kappa\wedge t}^{(i+1)\kappa\wedge t}\left[f(\bar{X}(i\kappa),\bar{X}(i\kappa-D),Z(s/\epsilon_1))-\bar{f}(\bar{X}(i\kappa),\bar{X}(i\kappa-D))\right]\mathrm{d}s\right|\\
&\leqslant\sup_{0\leqslant t\leqslant T}\left|\int_0^{(i+1)\kappa\wedge t}\left[f(\bar{X}(i\kappa),\bar{X}(i\kappa-D),Z(s/\epsilon_1))-\bar{f}(\bar{X}(i\kappa),\bar{X}(i\kappa-D))\right]\mathrm{d}s\right|\\
&\quad+\sup_{0\leqslant t\leqslant T}\left|\int_0^{i\kappa\wedge t}\left[f(\bar{X}(i\kappa),\bar{X}(i\kappa-D),Z(s/\epsilon_1))-\bar{f}(\bar{X}(i\kappa),\bar{X}(i\kappa-D))\right]\mathrm{d}s\right|\\
&\leqslant 2\sup_{0\leqslant t\leqslant (i+1)\kappa}\left|\int_0^{t}\left[f(\bar{X}(i\kappa),\bar{X}(i\kappa-D),Z(s/\epsilon_1))-\bar{f}(\bar{X}(i\kappa),\bar{X}(i\kappa-D))\right]\mathrm{d}s\right|\\
&=2\sup_{0\leqslant t\leqslant (i+1)\kappa}\epsilon_1\left|\int_0^{t/\epsilon_1}\left[f(\bar{X}(i\kappa),\bar{X}(i\kappa-D),Z(s))-\bar{f}(\bar{X}(i\kappa),\bar{X}(i\kappa-D))\right]\mathrm{d}s\right|.
\end{aligned} \tag{B5}$$

By the Birkhoff ergodic theorem and Theorem 4.35[2)], we obtain

$$\lim_{\epsilon_1\to 0}\sup_{0\leqslant t\leqslant (i+1)\kappa}\epsilon_1\left|\int_0^{t/\epsilon_1}\left[f(\bar{X}(i\kappa),\bar{X}(i\kappa-D),Z(s))-\bar{f}(\bar{X}(i\kappa),\bar{X}(i\kappa-D))\right]\mathrm{d}s\right|=0,\quad \text{a.s.,}$$

which combining with (B4) and (B5) gives that for any integer $n>0$,

$$\lim_{\epsilon_1\to 0}\sup_{0\leqslant t\leqslant T}\left|\int_0^t\left[f\big(\bar{X}^n(s),\bar{X}^n(s-D),Z(s/\epsilon_1)\big)-\bar{f}\big(\bar{X}^n(s),\bar{X}^n(s-D)\big)\right]\mathrm{d}s\right|=0,\quad \text{a.s.} \tag{B6}$$

By (B3), (B6), and

$$\lim_{n\to\infty}\sup_{-D\leqslant t\leqslant T}\left|\bar{X}(t)-\bar{X}^n(t)\right|=0,$$

we have

$$\lim_{\epsilon_1\to 0}\sup_{0\leqslant t\leqslant T}\left|\int_0^t\left[f\big(\bar{X}(s),\bar{X}(s-D),Z(s/\epsilon_1)\big)-\bar{f}\big(\bar{X}(s),\bar{X}(s-D)\big)\right]\mathrm{d}s\right|=0,\quad \text{a.s.}$$

The proof is completed.

Appendix C Proof of Theorem 3

Proof. To verify whether the algorithm can make the vehicles complete our goal, we define the following variables:

$$e_i^h(t)=\hat{x}_i(t)-\hat{c}(t)-(h_i-h^*), \tag{C1}$$

$$e^c(t)=\hat{c}(t)-x^*, \tag{C2}$$

where $\hat{x}_i(t)=x_i(t)-b_i\sin\big(\eta_i(t+D)\big)$, $\hat{c}(t)=\frac{1}{N}\sum_{i=1}^N\hat{x}_i(t)$, $e_i^h(t)$ is used to analyze whether the vehicles can achieve a formation during the source seeking process, and $e^c(t)$ is used to analyze whether the average position of the vehicles can converge to the signal source. By (1), (19), and (20), we obtain

$$\dot{e}_i^h(t)=k_1\xi_i(t)-\frac{k_1}{N}(\mathbf{1}_N^{\mathrm{T}}\otimes I_2)\xi(t), \tag{C3}$$

2) Anulova S V, Krylov N V, Liptser R S, et al. Probability Theory III: Stochastic Calculus. Berlin: Springer, 1998.

$$\dot{e}^c(t) = \frac{k_1}{N}(\mathbf{1}_N^{\mathrm{T}} \otimes I_2)\xi(t), \tag{C4}$$

$$\dot{\xi}_i(t) = k_1\left\{N_i(t)f_i(t)\xi_i(t) - k_2\sum_{j\in\mathcal{N}_i} a_{ij}\left(\xi_i(t)-\xi_j(t)\right)\right\} + k_3\Big\{M_i(t)f_i(t) - N_i(t)f_i(t)(h_i-h^*)$$
$$- k_2\sum_{j\in\mathcal{N}_i} a_{ij}\Big(e_i^h(t-D) - e_j^h(t-D) + b_i\sin\left(\chi_i(t/\varepsilon_i)\right) - b_j\sin\left(\chi_j(t/\varepsilon_j)\right)\Big) - \xi_i(t-D)\Big\}, \tag{C5}$$

where $\xi(t) = [\xi_1^{\mathrm{T}}(t),\dots,\xi_N^{\mathrm{T}}(t)]^{\mathrm{T}}$, $\chi_i(t) = [\chi_{i1}(t),\chi_{i2}(t)]^{\mathrm{T}}$, and $\chi_{ij}(t) = \eta_{ij}(\varepsilon_i t)$. For $i \in \{2,\dots,N\}$, we assume that $\varepsilon_i = \frac{\varepsilon_1}{c_i}$ with $c_i > 0$. Let $Z_{1j}(t) = \chi_{1j}(t)$, $Z_{ij}(t) = \chi_{ij}(c_i t)$ with $i \in \{2,\dots,N\}$ and $j \in \{1,2\}$. Then, Eqs. (C3)–(C5) become

$$\dot{e}_i^h(t) = k_1\xi_i(t) - \frac{k_1}{N}(\mathbf{1}_N^{\mathrm{T}} \otimes I_2)\xi(t), \tag{C6}$$

$$\dot{e}^c(t) = \frac{k_1}{N}(\mathbf{1}_N^{\mathrm{T}} \otimes I_2)\xi(t), \tag{C7}$$

$$\dot{\xi}_i(t) = k_1\left\{N_i(t)f_i(t)\xi_i(t) - k_2\sum_{j\in\mathcal{N}_i} a_{ij}\left(\xi_i(t)-\xi_j(t)\right)\right\} + k_3\Big\{M_i(t)f_i(t) - N_i(t)f_i(t)(h_i-h^*)$$
$$- k_2\sum_{j\in\mathcal{N}_i} a_{ij}\Big(e_i^h(t-D) - e_j^h(t-D) + b_i\sin\left(Z_i(t/\varepsilon_1)\right) - b_j\sin\left(Z_j(t/\varepsilon_1)\right)\Big) - \xi_i(t-D)\Big\}, \tag{C8}$$

where $Z_i(t) = [Z_{i1}(t), Z_{i2}(t)]^{\mathrm{T}}$, $M_i(t)$, $N_i(t)$, and $f_i(t)$ become

$$M_i(t) = \left[\frac{1}{b_{i1}G_0(q_{i1})}\sin\left(Z_{i1}(t/\varepsilon_1)\right), \frac{1}{b_{i2}G_0(q_{i2})}\sin\left(Z_{i2}(t/\varepsilon_1)\right)\right]^{\mathrm{T}},$$
$$N_i(t) = \begin{bmatrix} \frac{4(\sin^2(Z_{i1}(t/\varepsilon_1)) - G_0(q_{i1}))}{b_{i1}^2 G_0^2(\sqrt{2}q_{i1})} & \frac{\sin\left(Z_{i1}(t/\varepsilon_1)\right)\sin(Z_{i2}(t/\varepsilon_1))}{b_{i1}b_{i2}G_0(q_{i1})G_0(q_{i2})} \\ \frac{\sin\left(Z_{i1}(t/\varepsilon_1)\right)\sin(Z_{i2}(t/\varepsilon_1))}{b_{i1}b_{i2}G_0(q_{i1})G_0(q_{i2})} & \frac{4(\sin^2\left(Z_{i2}(t/\varepsilon_1)\right) - G_0(q_{i2}))}{b_{i2}^2 G_0^2(\sqrt{2}q_{i2})} \end{bmatrix},$$
$$f_i(t) = f^* + \frac{1}{2}\Big(e_i^h(t-D) + e^c(t-D) + (h_i-h^*) + b_i\sin\left(Z_i(t/\varepsilon_1)\right)\Big)^{\mathrm{T}} H\Big(e_i^h(t-D)$$
$$+ e^c(t-D) + (h_i-h^*) + b_i\sin\left(Z_i(t/\varepsilon_1)\right)\Big).$$

According to [32], $\{\chi_{ij}(t), t \geqslant 0\}$ is an Ornstein-Uhlenbeck (OU) process, which is ergodic with invariant distribution $\mu_{ij}(\mathrm{d}v) = \frac{1}{\sqrt{\pi}q_{ij}}\mathrm{e}^{-v^2/q_{ij}^2}\mathrm{d}v$. Meanwhile, all the OU processes are mutually independent. Then, the process $(Z(t), t \geqslant 0)$ is ergodic with the invariant distribution $\mu_{11} \times \mu_{12} \times \cdots \times \mu_{Nl} \times \mu_{N2}$, where $Z(t) = [Z_{11}(t), Z_{12}(t),\dots,Z_{N1}(t), Z_{N2}(t)]^{\mathrm{T}}$. Thus, based on the definition of (10), we can calculate the average system of system (C6)–(C8) as follows:

$$\dot{\bar{e}}_i^h(t) = k_1\bar{\xi}_i(t) - \frac{k_1}{N}(\mathbf{1}_N^{\mathrm{T}} \otimes I_2)\bar{\xi}(t), \tag{C9}$$

$$\dot{\bar{e}}^c(t) = \frac{k_1}{N}(\mathbf{1}_N^{\mathrm{T}} \otimes I_2)\bar{\xi}(t), \tag{C10}$$

$$\dot{\bar{\xi}}_i(t) = k_1\left\{H\bar{\xi}_i(t) - k_2\sum_{j\in\mathcal{N}_i} a_{ij}\left(\bar{\xi}_i(t)-\bar{\xi}_j(t)\right)\right\} + k_3\Big\{H\left(\bar{e}_i^h(t-D) + \bar{e}^c(t-D)\right)$$
$$- k_2\sum_{j\in\mathcal{N}_i} a_{ij}\left(\bar{e}_i^h(t-D) - \bar{e}_j^h(t-D)\right) - \bar{\xi}_i(t-D)\Big\}, \tag{C11}$$

where $\bar{\xi}(t) = [\bar{\xi}_1^{\mathrm{T}}(t),\dots,\bar{\xi}_N^{\mathrm{T}}(t)]^{\mathrm{T}}$, $\bar{\xi}_i(\theta) = \xi_i(\theta) = \varphi_i(\theta)$ when $\theta \in [-D, 0]$. Let $\bar{e}^h(t) = [\bar{e}_1^{h\mathrm{T}}(t),\dots,\bar{e}_N^{h\mathrm{T}}(t)]^{\mathrm{T}}$. Then, Eqs. (C9)–(C11) can be reduced to the much more condensed form:

$$\dot{\bar{e}}^h(t) = k_1\left(I_{2N} - \frac{1}{N}\left(\mathbf{1}_N \otimes \mathbf{1}_N^{\mathrm{T}} \otimes I_2\right)\right)\bar{\xi}(t), \tag{C12}$$

$$\dot{\bar{e}}^c(t) = \frac{k_1}{N}(\mathbf{1}_N^{\mathrm{T}} \otimes I_2)\bar{\xi}(t), \tag{C13}$$

$$\dot{\bar{\xi}}(t) = k_1\Big\{(I_N \otimes H) - k_2(\mathcal{L} \otimes I_2)\Big\}\bar{\xi}(t) + k_3\Big\{(I_N \otimes H)\left(\bar{e}^h(t-D)\right.$$
$$\left.+ \mathbf{1}_N \otimes \bar{e}^c(t-D)\right) - k_2(\mathcal{L} \otimes I_2)\bar{e}^h(t-D) - \bar{\xi}(t-D)\Big\}. \tag{C14}$$

For analyzing the stability of the system (C12)–(C14), we define the following error variable:

$$\zeta(t) = (I_N \otimes H)\left(\bar{e}^h(t) + \mathbf{1}_N \otimes \bar{e}^c(t)\right) - k_2(\mathcal{L} \otimes I_2)\bar{e}^h(t) - \bar{\xi}(t),$$

and it satisfies

$$\dot{\zeta}(t) = -k_3\zeta(t-D). \tag{C15}$$

Meanwhile, Eqs. (C12)–(C14) can be converted to

$$\dot{\bar{e}}^h(t) = k_1G\bar{e}^h(t) - k_1B\zeta(t), \tag{C16}$$

$$\dot{\bar{e}}^c(t) = k_1H\bar{e}^c(t) - \frac{k_1}{N}\big(\mathbf{1}_N^{\mathrm{T}} \otimes I_2\big)\zeta(t), \tag{C17}$$

$$\dot{\bar{\xi}}(t) = k_1G\bar{\xi}(t) + k_3\zeta(t-D), \tag{C18}$$

where $G = (I_N \otimes H) - k_2\big(\mathcal{L} \otimes I_2\big)$ and $B = I_{2N} - \frac{1}{N}(\mathbf{1}_N \otimes \mathbf{1}_N^{\mathrm{T}} \otimes I_2)$. The solutions of (C16) and (C17) are

$$\bar{e}^h(t) = \exp\big(k_1Gt\big)\bar{e}^h(0) - k_1\int_0^t \exp\big\{k_1G(t-s)\big\}B\zeta(s)\mathrm{d}s,$$

$$\bar{e}^c(t) = \exp\big(k_1Ht\big)\bar{e}^c(0) - \frac{k_1}{N}\int_0^t \exp\big\{k_1H(t-s)\big\}\big(\mathbf{1}_N^{\mathrm{T}} \otimes I_2\big)\zeta(s)\mathrm{d}s.$$

Since the communication graph is connected and undirected, $\mathcal{L}$ is a symmetric positive semi-definite matrix[3)]. And beyond that, H is a symmetrical negative definite matrix. Therefore, G is a symmetrical negative definite matrix. Let $\lambda_0 = \lambda_{\min}(-G)$ and $\lambda_1 = \lambda_{\min}(-H)$. Then we can know that $\exp\{-k_1\lambda_0t\}$ is the largest eigenvalue of $\exp\{k_1Gt\}$ and $\exp\{-k_1\lambda_1t\}$ is the largest eigenvalue of $\exp\{k_1Ht\}$ for $t > 0$. Then we have

$$\begin{aligned}
\left|\bar{e}^h(t)\right| &\leqslant \exp\big\{-k_1\lambda_0t\big\}\left|\bar{e}^h(0)\right| + k_1\int_0^t \exp\big\{-k_1\lambda_0(t-s)\big\}\big|B\zeta(s)\big|\mathrm{d}s \\
&\leqslant \exp\big\{-k_1\lambda_0t\big\}\left|\bar{e}^h(0)\right| + k_1\int_0^t \exp\big\{-k_1\lambda_0(t-s)\big\}\big|\zeta(s)\big|\mathrm{d}s,
\end{aligned} \tag{C19}$$

$$\begin{aligned}
|\bar{e}^c(t)| &\leqslant \exp\big\{-k_1\lambda_1t\big\}|\bar{e}^c(0)| + \frac{k_1}{N}\int_0^t \exp\big\{-k_1\lambda_1(t-s)\big\}\big|\big(\mathbf{1}_N^{\mathrm{T}} \otimes I_2\big)\zeta(s)\big|\mathrm{d}s \\
&\leqslant \exp\big\{-k_1\lambda_1t\big\}|\bar{e}^c(0)| + \frac{k_1}{\sqrt{N}}\int_0^t \exp\big\{-k_1\lambda_1(t-s)\big\}\big|\zeta(s)\big|\mathrm{d}s.
\end{aligned} \tag{C20}$$

It is not hard to see that the dynamics for $\bar{e}^h(t)$ and $\bar{e}^c(t)$ are exponentially stable if system (C15) is exponentially stable. Similar to [25], we construct the following Lyapunov functional:

$$V(t) = V_1(t) + V_2(t),$$

and

$$V_1(t) = \frac{1}{2}\zeta^{\mathrm{T}}(t)\zeta(t), \quad V_2(t) = \gamma k_3^3D\int_{t-2D}^t\int_\tau^t V_1(s)\mathrm{d}s\mathrm{d}\tau,$$

where $\gamma > 2$ is a constant. Along the solution of the system (C15), the derivative of $V_1(t)$ is given by

$$\begin{aligned}
\dot{V}_1(t) &= \zeta^{\mathrm{T}}(t)\big(-k_3\zeta(t-D)\big) \\
&= \zeta^{\mathrm{T}}(t)\big[-k_3\zeta(t) + k_3\big(\zeta(t) - \zeta(t-D)\big)\big] \\
&= -2k_3V_1(t) + k_3\zeta^{\mathrm{T}}(t)\int_{t-D}^t \dot{\zeta}(s)\mathrm{d}s \\
&= -2k_3V_1(t) + k_3\zeta^{\mathrm{T}}(t)\int_{t-D}^t \big(-k_3\zeta(s-D)\big)\mathrm{d}s \\
&= -2k_3V_1(t) - k_3^2\zeta^{\mathrm{T}}(t)\int_{t-2D}^{t-D} \zeta(s)\mathrm{d}s \\
&= -2k_3V_1(t) - k_3^2\int_{t-2D}^{t-D} \zeta^{\mathrm{T}}(t)\zeta(s)\mathrm{d}s.
\end{aligned}$$

Using the Cauchy-Buniakowsky-Schwarz inequality and integral inequality, we have

$$\begin{aligned}
\dot{V}_1(t) &\leqslant -2k_3V_1(t) + k_3^2\int_{t-2D}^{t-D} |\zeta(t)||\zeta(s)|\mathrm{d}s \\
&\leqslant -2k_3V_1(t) + k_3^2\int_{t-2D}^{t} |\zeta(t)||\zeta(s)|\mathrm{d}s
\end{aligned}$$

3) Godsil C, Royle G F. Algebraic Graph Theory. Berlin: Springer, 2001.

$$= -2k_3V_1(t) + \sqrt{k_3}|\zeta(t)| \cdot k_3^{\frac{3}{2}} \int_{t-2D}^{t} |\zeta(s)|\mathrm{d}s.$$

By the sum of squares inequality and Hölder inequality, we have

$$\begin{aligned}
\dot{V}_1(t) &\leqslant -2k_3V_1(t) + \frac{1}{2}k_3\zeta^{\mathrm{T}}(t)\zeta(t) + \frac{1}{2}k_3^3\left(\int_{t-2D}^{t}|\zeta(s)|\mathrm{d}s\right)^2 \\
&\leqslant -2k_3V(t) + \frac{1}{2}k_3\zeta^{\mathrm{T}}(t)\zeta(t) + \frac{1}{2}k_3^3\int_{t-2D}^{t}\zeta^{\mathrm{T}}(s)\zeta(s)\mathrm{d}s \cdot 2D \\
&= -2k_3V_1(t) + k_3V_1(t) + 2k_3^3D\int_{t-2D}^{t}V(s)\mathrm{d}s \\
&= -k_3V_1(t) + 2k_3^3D\int_{t-2D}^{t}V_1(s)\mathrm{d}s. \qquad (\mathrm{C21})
\end{aligned}$$

Along the solution of the system (C15), the derivative of $V_2(t)$ is given by

$$\begin{aligned}
\dot{V}_2(t) &= \gamma k_3^3D\left\{\int_{t}^{t}V_1(s)\mathrm{d}s - \int_{t-2D}^{t}V_1(s)\mathrm{d}s + \int_{t-2D}^{t}V_1(t)\mathrm{d}\tau\right\} \\
&= -\gamma k_3^3D\int_{t-2D}^{t}V_1(s)\mathrm{d}s + 2\gamma k_3^3D^2V_1(t). \qquad (\mathrm{C22})
\end{aligned}$$

Combining (C21) and (C22), we know that the derivative of $V(t)$ satisfies

$$\begin{aligned}
\dot{V}(t) &\leqslant -k_3V_1(t) + 2k_3^3D\int_{t-2D}^{t}V_1(s)\mathrm{d}s - \gamma k_3^3D\int_{t-2D}^{t}V_1(s)\mathrm{d}s + 2\gamma k_3^3D^2V_1(t) \\
&= -k_3\big(1 - 2\gamma k_3^2D^2\big)V_1(t) - \big(\gamma - 2\big)k_3^3D\int_{t-2D}^{t}V_1(s)\mathrm{d}s.
\end{aligned}$$

Since

$$\int_{t-2D}^{t}\int_{\tau}^{t}V_1(s)\mathrm{d}s\mathrm{d}\tau \leqslant 2D\int_{t-2D}^{t}V_1(s)\mathrm{d}s,$$

we have

$$\begin{aligned}
\dot{V}(t) &\leqslant -k_3\big(1 - 2\gamma k_3^2D^2\big)V_1(t) - \frac{\gamma-2}{2}k_3^3\int_{t-2D}^{t}\int_{\tau}^{t}V_1(s)\mathrm{d}s\mathrm{d}\tau \\
&= -k_3\big(1 - 2\gamma k_3^2D^2\big)V_1(t) - \frac{\gamma-2}{2\gamma D}V_2(t) \\
&\leqslant -\rho V(t),
\end{aligned}$$

where $\rho = \min\{k_3\big(1 - 2\gamma k_3^2D^2\big), \frac{\gamma-2}{2\gamma D}\} > 0$. From $V_1(t) \leqslant V(t) = V(0) + \int_0^t \dot{V}(s)\mathrm{d}s \leqslant V(0) + \int_0^t -\rho V_1(s)\mathrm{d}s$, we obtain $\dot{V}_1(t) \leqslant -\rho V_1(t)$, which means $V_1(t) \leqslant V_1(0)\exp\{-\rho t\}$, namely,

$$|\zeta(t)| \leqslant |V(0)|\exp\Big\{-\frac{\rho}{2}t\Big\}, \quad \forall t \geqslant 0. \qquad (\mathrm{C23})$$

Therefore, the solution of system (C15) globally exponentially converges to zero. When k_1 satisfies $k_1\lambda_0 \neq \frac{\rho}{2}$ and $k_1\lambda_1 \neq \frac{\rho}{2}$, Eqs. (C19) and (C20) satisfy

$$\begin{aligned}
\left|\bar{e}^h(t)\right| &\leqslant \exp\big\{-k_1\lambda_0t\big\}\left|\bar{e}^h(0)\right| + k_1\int_0^t\exp\big\{-k_1\lambda_0(t-s)\big\}|V(0)|\exp\Big\{-\frac{\rho}{2}s\Big\}\mathrm{d}s, \\
&= \left|\bar{e}^h(0)\right|\exp\big\{-k_1\lambda_0t\big\} + \frac{k_1|V(0)|}{\frac{\rho}{2} - k_1\lambda_0}\Big\{\exp\big\{-k_1\lambda_0t\big\} - \exp\Big\{-\frac{\rho}{2}t\Big\}\Big\} \\
&\leqslant \mu_0\exp\big\{-\nu_0t\big\}, \\
|\bar{e}^c(t)| &\leqslant \exp\big\{-k_1\lambda_1t\big\}|\bar{e}^c(0)| + \frac{k_1}{\sqrt{N}}\int_0^t\exp\big\{-k_1\lambda_1(t-s)\big\}|V(0)|\exp\Big\{-\frac{\rho}{2}s\Big\}\mathrm{d}s \\
&= |\bar{e}^c(0)|\exp\big\{-k_1\lambda_1t\big\} + \frac{k_1|V(0)|}{\sqrt{N}\big(\frac{\rho}{2} - k_1\lambda_1\big)}\Big\{\exp\big\{-k_1\lambda_1t\big\} - \exp\Big\{-\frac{\rho}{2}t\Big\}\Big\} \\
&\leqslant \mu_1\exp\big\{-\nu_1t\big\},
\end{aligned}$$

where $\nu_0 = k_1\lambda_0 \wedge \frac{\rho}{2}$, $\mu_0 = |\bar{e}^h(0)| + \frac{k_1|V(0)|}{|k_1\lambda_0 - \frac{\rho}{2}|}$, $\nu_1 = k_1\lambda_1 \wedge \frac{\rho}{2}$, and $\mu_1 = |\bar{e}^c(0)| + \frac{k_1|V(0)|}{\sqrt{N}|k_1\lambda_1 - \frac{\rho}{2}|}$. Then by Theorem 2, for any $\delta > 0$, we have

$$\lim_{\varepsilon_1\to 0}\ \inf\{t \geqslant 0 : |e^h(t)| > \mu_0\exp\big\{-\nu_0t\big\} + \delta\} = +\infty, \quad \text{a.s.}, \qquad (\mathrm{C24})$$

$$\lim_{\varepsilon_1 \to 0} \inf\{t \geqslant 0 : |e^c(t)| > \mu_1 \exp\big\{-\nu_1 t\big\} + \delta\} = +\infty, \quad \text{a.s.} \tag{C25}$$

For $i \in \mathcal{V}$, by (C1) and (C2), we know

$$x_i(t) - c(t) - h_i + h^* = e_i^h(t) + b_i \sin\big(\eta_i(t+D)\big) - \frac{1}{N}\sum_{i=1}^{N} b_i \sin\big(\eta_i(t+D)\big),$$

$$c(t) - x^* = e^c(t) + \frac{1}{N}\sum_{i=1}^{N} b_i \sin\big(\eta_i(t+D)\big).$$

Combining with (C24) and (C25), we have

$$\lim_{\varepsilon_1 \to 0} \inf\left\{t \geqslant 0 : \big|x(t) - \mathbf{1}_N \otimes c(t) - h + \mathbf{1}_N \otimes h^*\big| > \mu_0 \exp\big\{-\nu_0 t\big\} + \delta + \sqrt{\frac{N-1}{N}}\sqrt{\sum_{i=1}^{N}\big(b_{i1}^2 + b_{i2}^2\big)}\right\} = +\infty, \quad \text{a.s.,} \tag{C26}$$

$$\lim_{\varepsilon_1 \to 0} \inf\left\{t \geqslant 0 : \big|c(t) - x^*\big| > \mu_1 \exp\big\{-\nu_1 t\big\} + \delta + \frac{1}{\sqrt{N}}\sqrt{\sum_{i=1}^{N}\big(b_{i1}^2 + b_{i2}^2\big)}\right\} = +\infty, \quad \text{a.s.} \tag{C27}$$

The proof is completed.